NTNU – Trondheim
Norwegian University of
Science and Technology

# Marine palaeoproductivity in the Blodøks Formation of the North Sea.

Frederick Owusu

Petroleum Geosciences
Submission date: June 2015
Supervisor: Maarten Felix, IGB

Norwegian University of Science and Technology
Department of Geology and Mineral Resources Engineering

# ACKNOWLEDGEMENT

I wish to express my sincere gratitude to the Norwegian Government for the Quota Scheme scholarship that has made it possible to pursue my Master's degree in Petroleum Geosciences. Many thanks also go to my supervisor Dr. Maarten Felix of the Department of Geology and Mineral Resource Engineering for his time, patience, guidance and advice in writing this thesis.

Special thanks also go to Professor Stephen Lippard for his advice throughout the course, my family and fellow colleagues who contributed in one way or the other for a successful study. I appreciate everything.

## ABSTRACT

Organic carbon accumulations within sediments are linked to several factors such as sedimentation rates, primary productivity rates, water depths and terrestrial inputs. In this study, palaeoproductivity was estimated with two equations used to calculate total organic carbon: the Müller and Suess (1979) equation and the Stein (1986) equation. The palaeoproductivity calculations used both measured data gathered from multiple cores, and calculated input data. The measured total organic carbon values within the Blodøks Formation ranged from 0.1-2.93wt%. The sedimentation rates were determined to be low, ranging from 0.08-12.16(cm/1000yr), and dry bulk density was estimated as 0.675g/cm$^3$. The Stein (1986) equation gives lower estimations of palaeoproductivity than the results obtained from the Müller and Suess (1979) equation. The input data and estimated primary productivity results of the Stein (1986) equation were plotted to show the spatial distributions. The main influences on the accumulation of organic carbon within the Blodøks Formation are primary productivity rates and anoxic conditions at the water bottom. The accumulated organic carbon was dominated by residuals of both marine and terrestrial origin. Regionally, palaeo-conditions from the North Sea to the Norwegian Sea during the time interval did not vary much. This argument is supported by similar organic carbon accumulations, primary productivity rates, sedimentation rates from the Blodøks (Svarte and Hidra Blodøks) in the North Sea to its equivalent the Blålange Formation in the Norwegian Sea. Anoxic conditions are inferred to be the primary control on the preservation of organic carbon in the Langebarn and Knitvos Formations in the Norwegian Sea during the Cretaceous period and locally primary productivity rate.

## Table of Contents

## List of Figures

## List of Tables

## List of Equations



## Appendix

## 1.0 Introduction

Phytoplankton undoubtedly forms the major primary producers in the marine ecosystems, accounting for about 90% of organic carbon production through the processes of photosynthesis (Allen and Allen, 2013). The production of organic carbon is dependent on several factors such as light, nutrient supply such as nitrates and phosphates, temperature, turbidity and salinity (Allen and Allen, 2013).

The rate, distribution and types of primary productivity generated debate among several authors until the reconstruction of ocean productivity from sedimentary records made enormous contributions to this discussion (Berger and Herguera, 1992). Marine palaeoproductivity can be estimated from several equations such as the Müller and Suess (1979) equation, the Stein (1986) equation or a combination of both equations. Each of these equations has its own limitations. Depending on the types of equations used, large differences in palaeoproductivities could result in different interpretations of depositional environments. The weakness of these equations is the neglect of terrestrial input thereby correlating primary productivities to total organic carbon instead of marine organic carbon (Felix, 2014).

The preservation of organic carbon in sediments is favoured by anoxic conditions because processes such as oxidation, bacterial degradation or scavenging by fauna are inhibited. Anoxic conditions may be developed in areas of high productivity where the consumption of oxygen exceeds its production and stratification in the water column due to temperature or density contrasts (Demaison and Moore, 1980). The Aptian-Albian, Cenomanian to early Turonian and Coniacian to Santonian period are considered as the oceanic anoxic events in the Cretaceous (Jenkyns, 1980). The Aptian-Albian and Cenomanian to early Turonian are believed to be associated with rich depositions of organic carbon (Schlanger and Jenkyns, 1976).

Research studies conducted by Barrett (1998) on the Cenomanian-Turonian Black Band Formation in UK attributed the enhanced organic carbon within the formation to the anoxic conditions and increased primary productivity. The Black Band Formation in the UK is suggested as the equivalence of the Blodøks Formation (Plenus Marl) of the North Sea (Deegan and Scull, 1977). This formation is also enriched in organic carbon (Jenkyns, 1985) but causes of this enrichment have not been studied.

Due to the limited palaeoproductivity research study in the Cenomanian-Turonian period of the North Sea, the Blodøks Formation and its equivalent members in the Blålange Formation in the Norwegian Sea present a good study case for this project because these formations were deposited during the anoxic events of the late Cenomanian to early Turonian period. This project can serve as a backbone for investigating the regional variations in the primary productivity from the Norwegian shelf to the UK sector as it relates the primary productivity rates to the palaeo-environmental conditions during the time interval.

Comparison of the Blodøks Formation with its equivalent, the Blålange in the Norwegian Sea is useful because the Blodøks Formation is deposited between carbonate formations unlike the Blålange Formation which is bounded by clastic deposits, and so this can be used in determining the vertical changes in palaeoproductivity trend in the clastics over time. This project takes into account input data such as total organic carbon, sedimentation rates, dry bulk density and water depths. The input data are incorporated into Matlab codes to generate a model to better understand the spatial distributions.

## 1.1 Aims and objectives

The aims and objective of this project are as follows:

1. Collect and gather data/information from public data sources such as Norwegian Petroleum Directorates online factpages, reports and published literature.
2. Determine marine palaeoproductivity using both measured values from the Cretaceous Blodøks Formation cores and calculated input data.
3. Determine the main influences on the preservation of organic carbon within the Blodøks Formation.
4. Determine the lateral distribution of organic carbon from the North Sea to its equivalent in the Norwegian Sea.
5. Determine the influences on the accumulated organic carbon from the stratigraphically lower to higher formations in the Norwegian Sea.

## 2.0 Geographical distribution and lithology

### 2.1 Geographical distribution of the Blodøks Formation

The Blodøks Formation is a sub-division of the parent lithostratigraphic unit, the Shetland Group in the North Sea. It belongs to the late Cenomanian to early Turonian (Isaksen and Tonstad, 1989). It is widely distributed throughout the southern and central parts of the North Sea and reaches a maximum thickness of about 28m thick in the UK sector of the North Sea (Deegan and Scull, 1977) and about 120m thick in the Norwegian sector (Surlyk et al., 2003). The Blodøks Formation is absent on local structural highs such as the Sørvestlandet High (Figure 1), the Utsira, Mandal, Jæren and Sele Highs, Grensen High and above salt diapirs (Isaksen and Tonstad, 1989).

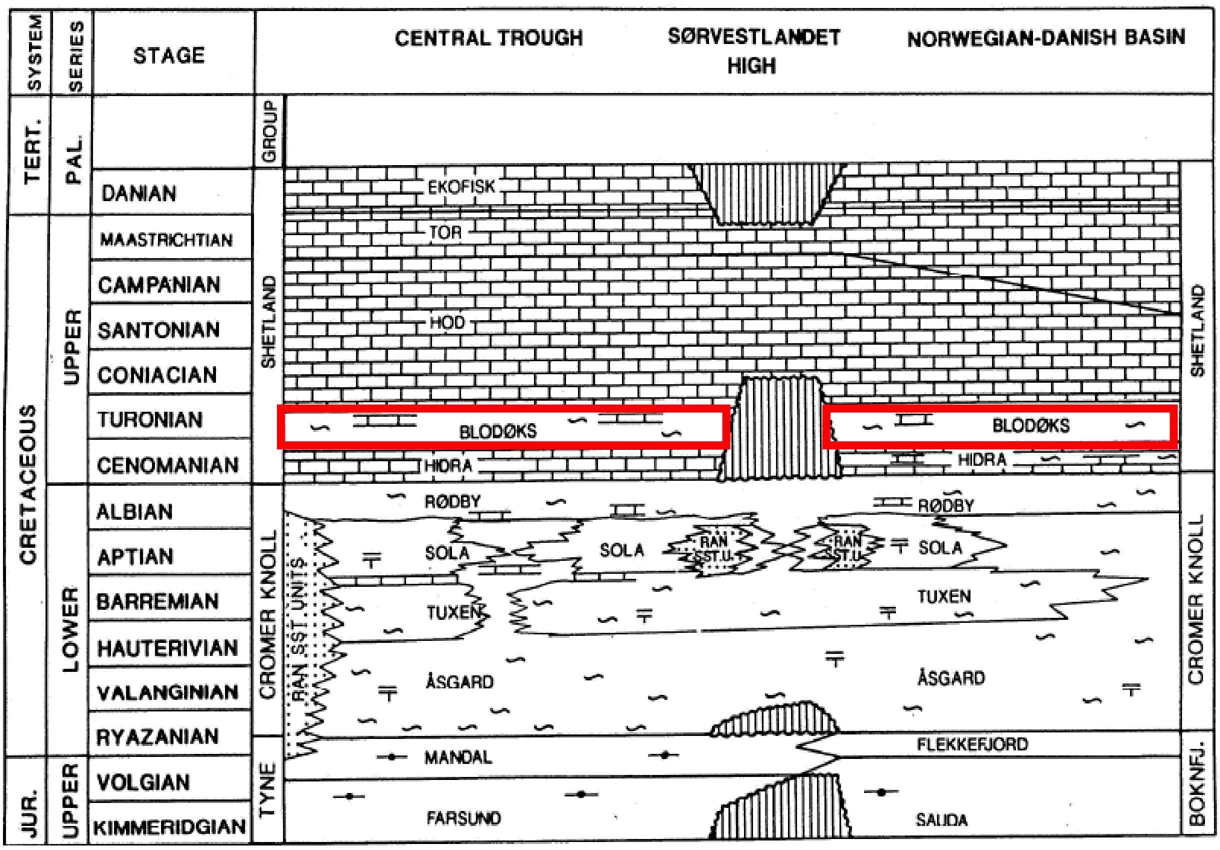


Figure 1 The lateral distribution of the Blodøks Formation (red outline) from the central trough to the Norwegian Danish basins of the North Sea (Isaksen and Tonstad, 1989).

### 2.1.1 Lithology of the Blodøks Formation

The Blodøks Formation is composed of black mudstones overlain by red, green, weakly to moderately calcareous grey mudstones and argillaceous limestones (Surlyk et al., 2003). In the central North Sea, it consists of marls, limestones and chalky limestones (Isaksen and Tonstad, 1989). It is referred to as the Plenus Marl formation by Deegan and Scull (1977) as shown in Figure 2.

| SERIES | STAGE | Deegan & Scull (1977) | | | Present subdivision | | | |
|---|---|---|---|---|---|---|---|---|
| | | Chalk Gp. | | Shetland Gp. | Shetland Gp. | | | |
| | | W Central North Sea E | | W Northern North Sea E | W Central North Sea E | | W Northern North Sea E | |
| Paleocene | Thanetian | Maureen Fm./ Unnamed unit | | | Lista / Våle / Maureen /Ty Fm. | | | |
| Paleocene | Danian | Ekofisk Fm. | | Fm. F | Ekofisk Fm. | | | |
| Upper Cretaceous | Maastrichtian | Tor Fm. | | Fm. E | Tor Fm. | | Jorsalfare Fm. | Hardråde Fm. |
| Upper Cretaceous | Campanian | Flounder Fm. | Hod Fm. | Fm. D | Flounder Fm. | Hod Fm. | Kyrre Fm. | |
| Upper Cretaceous | Santonian | Flounder Fm. | Hod Fm. | Fm. D | Flounder Fm. | Hod Fm. | Kyrre Fm. | |
| Upper Cretaceous | Coniacian | Flounder Fm. | Hod Fm. | Fm. D | Flounder Fm. | Hod Fm. | Kyrre Fm. | |
| Upper Cretaceous | Turonian | Herring Fm. | Hod Fm. | Fm. C | Herring Fm. | Hod Fm. | Tryggvason Fm. | Unspec. |
| Upper Cretaceous | Turonian | Plenus Marl Fm. | | Fm. B | Blodøks Fm. | | | Unspec. |
| Upper Cretaceous | Cenomanian | Hidra Fm. | | Fm. A | Hidra Fm. | | Svarte Fm. | Unspec. |
| L.Cret. | Albian | Valhall/Rødby Fm. | | Unspec. unit | Rødby Fm. | | | |

Figure 2 The previous and present subdivision of the Upper Cretaceous (Isaksen and Tonstad, 1989).

## 2.2 Geographical distribution of the Blålange Formation

The Blålange Formation belongs to the late Cretaceous period in the Norwegian Sea. It consists of eight members of the age interval ranging from the Cenomanian to Coniacian. It is the equivalent of the upper parts of the Lange Formation defined by Dalland et al. (1988). It is geographically distributed in the Møre margin, Halten and Dønna Terrace areas and Vestfjorden basin area (Færseth and Lien, 2002). It is thicker towards the west (Halten and Dønna Terrace) and thinner in the Trøndelags Platform. It is over 1300m thick in the Møre and Vøring basin area (Swiecicki et al., 1998). It is underlain by the Langebarn Formation (Færseth and Lien, 2002) and overlain by the Knitvos Formation (Dalland et al., 1988).

### 2.2.1 Lithology of the Blålange Formation

The Blålange Formation is composed of mainly mudstones which are generally non-calcareous, medium dark grey to medium brown grey, subfissile to fissile, blocky with subordinate sandstones and siltstones as beds and limestones, dolomites and marls as stringers (Dalland et al., 1988).

## 3.0 Geological setting and depositional environment

### 3.1 Geological History of the Cretaceous Period in the North Sea

Prior to the late Cretaceous, the late Jurassic to early Cretaceous is associated with a late phase of extensional tectonics (rift) which resulted in the formation of rotated fault blocks and structural traps beneath the Viking and Central Grabens in the North Sea as shown in Figure 3 (Glennie and Underhill, 1998). This was followed by a post-rift thermal subsidence in the late (Upper) Cretaceous. This period was accompanied with a major rise in sea level (marine transgression) through which Cretaceous sediments were deposited onto the Jurassic formations. With the exception of the deeper parts of the rift where sedimentation was probably continuous, an unconformity known as the Base Cretaceous Uncomformity (BCU) occurs between the Jurassic and Cretaceous sequences (Faleide et al., 2010).

Faleide et al. (2010) subdivided the Cretaceous development in the northern North Sea into three stages:

1. Ryazanian to late Albian; This stage is associated with differential subsidence of the basin following the syn-rift period which contributed to the basin configuration and sediment distribution.
2. Cenomanian to late Turonian; This marks the period where sedimentation of the basin balanced or exceeded the subsidence rate.
3. Early Coniacian to early Paleocene; This characterises the mature post rift stage where subsidence of the basin ceased due to thermal equilibrium, therefore sedimentation was affected by extra-basinal processes.

The late Cretaceous marks a quiescent tectonic period in the North Sea (Isaksen and Tonstad, 1989). At the end of the Cretaceous period through to early Tertiary, the North Sea areas were subjected to tectonic inversions (uplift) related to the Alpine Orogeny to the south (Faleide et al., 2010).

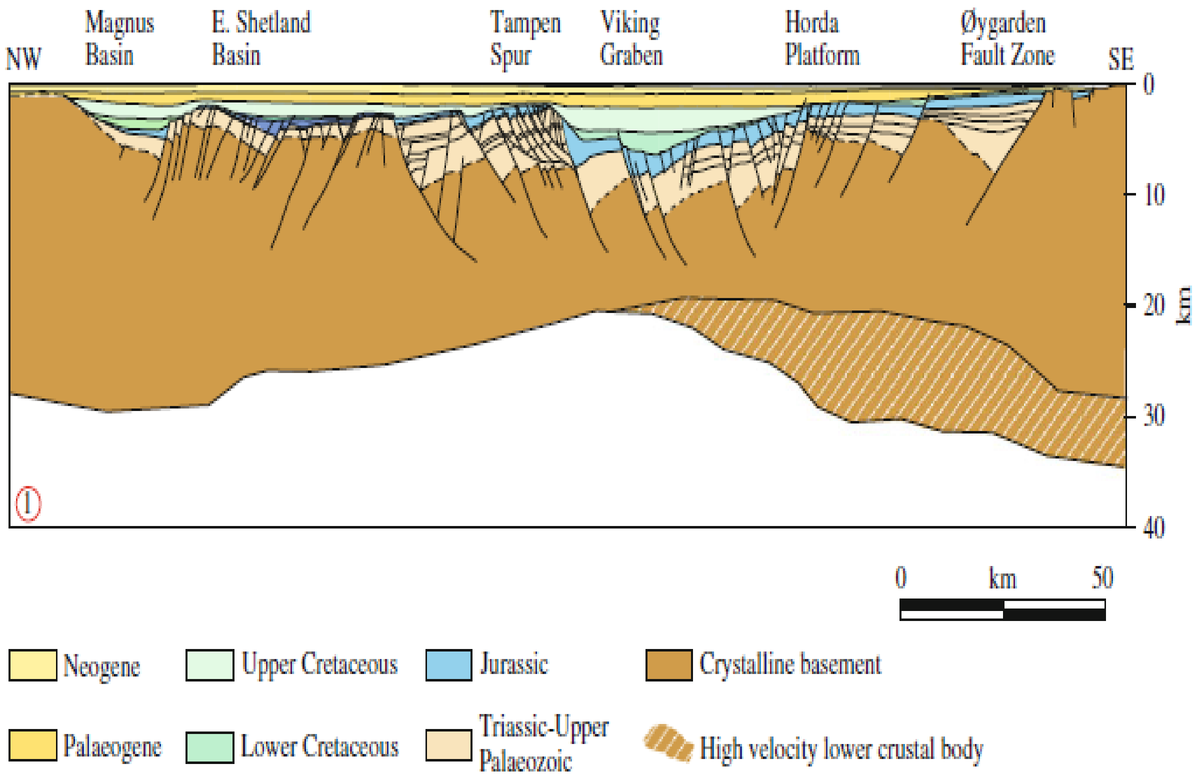


Figure 3 The basin configuration of the northern North Sea (Christiansson et al., 2000).

### 3.2 Depositional environment in the Cretaceous of the North Sea

Prior to the late Cretaceous, the Ryazanian period was characterised by a low-stand after which the sea level rose to an intermediate maximum in the Barremian period. This resulted in widespread deposition of shales and marls on the platforms and in deeper basins. Deposition ceased after the peak of the Barremian high-stand due to the drop of sea level which enhanced a deltaic progradation from transgressed land areas to the basins (Brekke et al., 2001). The Cromer Knoll Formation which was deposited during the early Cretaceous consists of shales, shallow to deep marine sandstones and sands. The shales vary from being oxidised (grey to reddish) to calcareous upwards (Faleide et al., 2010).

The late Cretaceous is characterised by a warm-temperate to subtropical climate, normal saline content of the sea water and relatively warm temperatures (Surlyk et al., 2003). According to Sørensen et al. (1992) the onset of the late Cretaceous coincided with acceleration of the global sea floor spreading rate which resulted in a major transgression of the North Sea areas. The sea level reached its peak in the late Cretaceous period and the supply of clastic sediments was cut off (Surlyk et al., 2003). In the southern and central North

Sea, clastic sedimentation into the basins was cut off (reduced) during the Cenomanian period and afterwards which resulted in the deposition of pure carbonates (Isaksen and Tonstad, 1989). Planktonic carbonate algae (coccolithoporids) dominated the sedimentation across the North Sea basins giving rise to depositions of pelagic chalk formations. The sea level reached a maximum in the middle of the Campanian and pure chalk formations were deposited from the Campanian to Maastrichtian period (Faleide et al., 2010).

The sedimentation of the chalk continued to the Danian (Paleocene) period (Faleide et al., 2010). The late Cretaceous deposits of the North Sea may be divided into two zones; the chalk province in the southern parts and the clastic province in the northern parts (Sørensen et al., 1992). The occurrence of a mudstone dominated sequence in the North indicates the source of terrigenous supply from the North (Hancock, 1990). Shales dominate the sequences along the northern parts of the Viking Graben (Faleide et al., 2010). The Blodøks Formation was deposited during anoxic conditions at the sea bottom (Hart and Leary, 1989).

## 4.0 Primary productivity, sources and preservation of organic carbons

### 4.1 Previous studies on productivity, sedimentation rates and organic carbon preservation

Various studies have been conducted by several authors to estimate marine palaeoproductivity both on a global and local scale. Earlier studies include Müller and Suess (1979) to determine productivity, sedimentation rates and organic matter content in the oceans and their influences on organic carbon preservation by analyses of samples from the Pacific Ocean, Atlantic Ocean and Baltic Sea. It was concluded in their studies that the sedimentation rate is related to the preservation of organic carbon. Suess (1980) determined the relation between primary productivity and downward flux of organic carbon by using sediment trap deployments in the world's oceans. It was suggested that the downward flux of organic carbon is directly proportional to primary productivity at the surface. Later works by Betzer et al. (1984) on a transect of the equator in the Pacific Ocean revealed, by analysing water samples collected within specific depths, that an increase in primary production to about 4-fold corresponds to an increase in downward flux of organic carbon to about 7-fold. A recent publication by Felix (2014) compared the equations used to calculate organic matter content and palaeoproductivity with present day measured data in which it was revealed that while the results of some equations showed consistency with measured data, other results were unreliable.

### 4.2 Primary productivity

Primary productivity is defined as the amount of organic carbon produced from the atmosphere or aquatic carbon dioxide via photosynthesis and/or chemosynthesis. In terms of primary productivity distributions, areas with the highest organic carbon productivity occur at the continental shelves, upwelling zones, estuaries, algal beds and reefs, and decrease towards the open ocean as shown in Table 1 (Woodwell et al., 1978; Nienhuis, 1981). The most productive zones within marine ecosystems are the photic zones which extend from the surfaces to depths of about 200m. On a global scale, maximum primary production occurs at mid latitude humid and equatorial latitude and the least in polar and tropical areas (Allen and Allen, 2013).

Table 1 Global net primary production (Woodwell et al., 1978; Nienhuis 1981).

| **Ecosystem type** | **Area ($10^6 km^2$)** | **Total net primary productivity** | | **Total plant mass of carbon $10^9 tC_{org}$** |
|---|---|---|---|---|
| | | **$10^9 tC_{org} yr^{-1}$** | **$gC_{org} m^{-2} yr^{-1}$** | |
| Marine ecosystems | 361.0 | 24.7 | 68.7 | 1.74 |
| Algal bed and reef | 0.6 | 0.7 | 1166.7 | 0.54 |
| Estuaries | 1.4 | 1.0 | 714.3 | 0.63 |
| Upwelling zones | 0.4 | 0.1 | 250.0 | 0.004 |
| Continental shelf | 26.6 | 4.3 | 161.6 | 0.12 |
| Open ocean | 332.0 | 18.7 | 56.3 | 0.45 |

### 4.3 Sources and supply of organic carbon

Marine (autochthonous) and terrestrial (allochthonous) organic carbon constitute the main types of organic carbon. In the oceans, the total organic carbon may comprise a component of both marine and terrestrial origin (Allen and Allen, 2013). Marine organic carbon (autochthonous) may undergo degradation in the water column or at the sediment surface prior to its burial within sediments depending on the water depth, sinking velocity and redox conditions. Hence the greater the sinking velocities, the lesser the transit time within the water column and degradation (Mann and Zweigel, 2008). Schlünz and Schneider (2000) estimated that about $430*10^{12}$g of terrestrial organic matter are transported into the oceans through rivers, ice berg (high latitude) and wind although quantitative estimations of the latter are difficult.  These terrestrial organic carbons are either remineralised or dispersed in the ocean from which it may settle and accumulate within sediments. About 10% constituting $43*10^{12} gCyear^{-1}$ is preserved in marine sediments.

Terrestrial (allochthonous) organic matter is prone to degradation during transportation prior to its deposition into the oceans; as such they are more resistant to further degradation compared to autochthonous organic matter which undergoes degradation through the water column (Hedges and Keil, 1995).  The transport distance influences the grain sizes and quality of allochthonous materials (Mann and Zweigel, 2008) except rapidly depositing systems such as turbidity currents which supply allochthonous materials to the deep sea (Degens et al., 1986). The sources of organic carbon in sediments can be determined from the hydrogen and oxygen indexes as shown in Table 2 (Jones, 1987). High hydrogen indexes are associated with marine organic carbon while low hydrogen index is associated with terrestrial organic carbon (Van Krevelen, 1984).

Table 2 Sources of organic matter based on hydrogen and oxygen index (Modified from Jones, 1987).

| **HI ($mgHC/gC_{org}$)** | **OI ($mgCO_2/gC_{org}$)** | **Sources** |
|---|---|---|
| 250 – 400 | 40 - 80 | Mixed (some oxidation) |
| 125 – 250 | 50 - 150 | Terrestrial (some oxidation) |
| 50 – 150 | 40 – 150+ | Reworked (oxidation) |
| < 50 | 20 – 200+ | Reworked (oxidation) |

### 4.4 Preservation of organic matter

The preservation of organic matter is dependent on several factors; while some are generally applicable to all environments, others are more restricted to specific environments (Canfield, 1994). These factors include organic carbon source, sediment grain size, water depths and sedimentation rate.

#### 4.4.1 Organic carbon source

Canfield (1994) suggested that the preservation of organic carbon is dependent on the amount of marine and terrestrial organic carbon. Thus, organic carbon of terrestrial origin (lignin) is less susceptible to degradation which increases the chances of being preserved compared to marine sources.

#### 4.4.2 Sediment grain size

Finer grain sizes such as clay have a higher potential of preserving organic matter due to lower permeability than coarse grains. Hence infiltration of oxygen into sediments is inhibited at shallow depths thereby reducing oxidation and other bacterial activities unlike coarse grains which are associated with relatively high depositional environments and tend to be oxygenated (Allen and Allen, 2013).

#### 4.4.3 Water depths

An increase in water depth increases the settling time of organic carbon from the water surfaces to the bottom which exposes the organic carbon to oxidation, scavenging fauna and bacterial degradation causing a reduction in carbon flux (Figure 4). Hence, shallow water depths are favourable for preservation of organic carbon due to less transit time in the water column (Betzer et al., 1984; Schwarzkopf, 1993; Allen and Allen, 2013). Schwarzkopf (1993) defined carbon flux as ‘the transport of organic carbon from the surficial layers (photic zones) to the seafloor’. Measurements of carbon data from sediment traps indicate that most of the organic carbon from the photic zones (export production) is recycled via direct oxidation or degradation (Weedon et al., 2004) with a greater percentage of export production being associated with coastal areas than with open oceans (Berger et al., 1989). Betzer et al. (1984) correlated carbon flux as a function of primary productivity and water depth as shown in equation 1 (Betzer et al., 1984):

$$C.F = 0.409WD - 0.628PP^{1.41} \quad (1)$$

where $C.F$ = carbon flux ($gC/m^2/a$), $WD$ = water depth (m), $PP$ = primary productivity ($gC/m^2/a$).

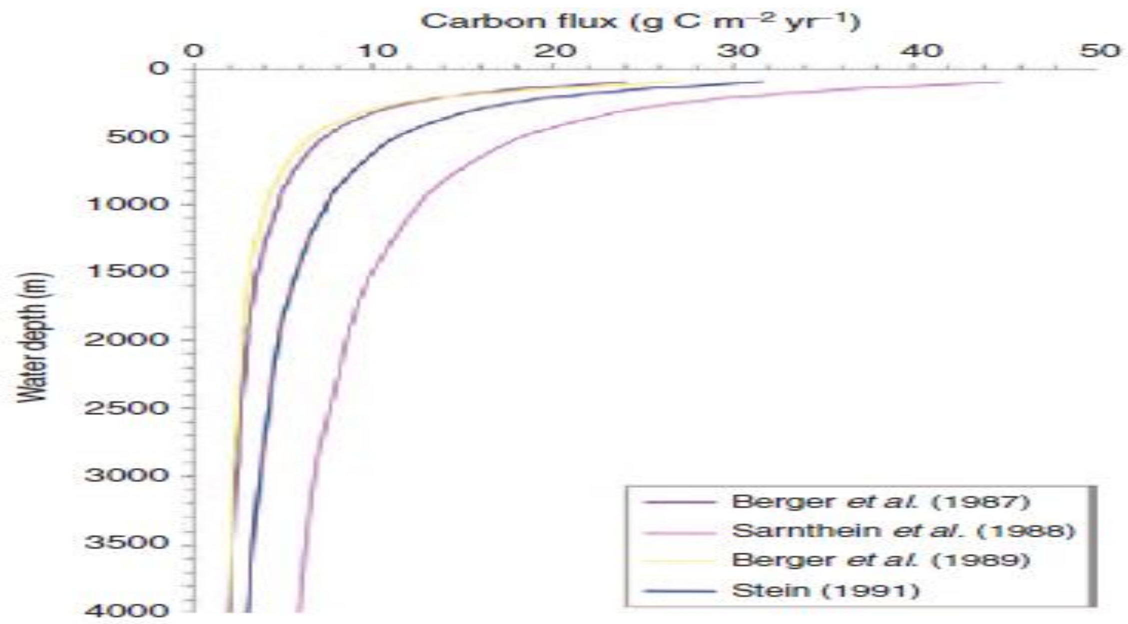


Figure 4 The carbon flux as a function of water depth using equations of Berger et al. (1987; 1989), Sarnthein et al. (1988) and Stein (1991) with a constant productivity (Mann and Zweigel, 2008).

### 4.4.4 Sedimentation rates

The rate at which sediments are being deposited affects the preservation of organic carbon. An increase in sedimentation rate increases the rate of burial of organic matter. This reduces exposure to oxidation and degradation by bacteria influences (Schwarzkopf, 1993; Allen and Allen, 2013). Tyson (1996) attributed the effects of sedimentation rates on total organic carbon to oxic conditions at the water bottom; linking low total organic carbon to oxic conditions and high total organic carbon to anoxic conditions. As seen in Figure 5, the total organic carbon increases with sedimentation rate until the burial efficiency reaches a maximum at which preservation is no longer dependent on sedimentation rate.

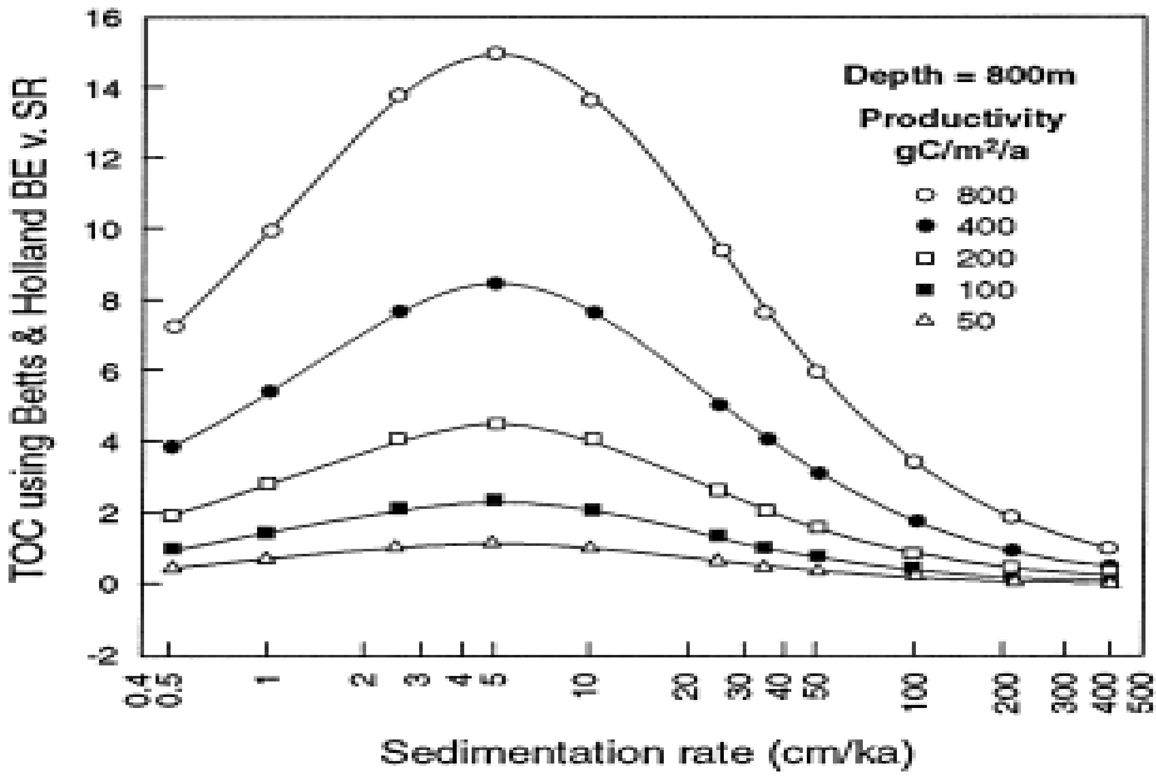


Figure 5 Total organic carbon (TOC) as a function of sedimentation rate at a fixed depth of 800m within a range of primary productivities (Tyson, 2001).

### 4.5 Burial efficiency

Betts and Holland (1991) defined burial efficiency as 'the ratio of organic carbon which is ultimately buried to the organic carbon which reaches the sediment water interface'. It is dependent on sedimentation rates.

$$log_{10}\left(\frac{BE}{100}\right) = \frac{1.39 * log_{10}SR}{log_{10}(SR+7.9)} + 0.34 \quad (2)$$

where $BE$ = burial efficiency, $S.R$ = sedimentation rate (cm/ka).

From Figure 6, initially burial efficiency increases with sedimentation rates until a point where it is no longer dependent on sedimentation rates and becomes constant. Tyson (2001) suggested that burial efficiency is most likely to be higher in permanently anoxic bottom water.

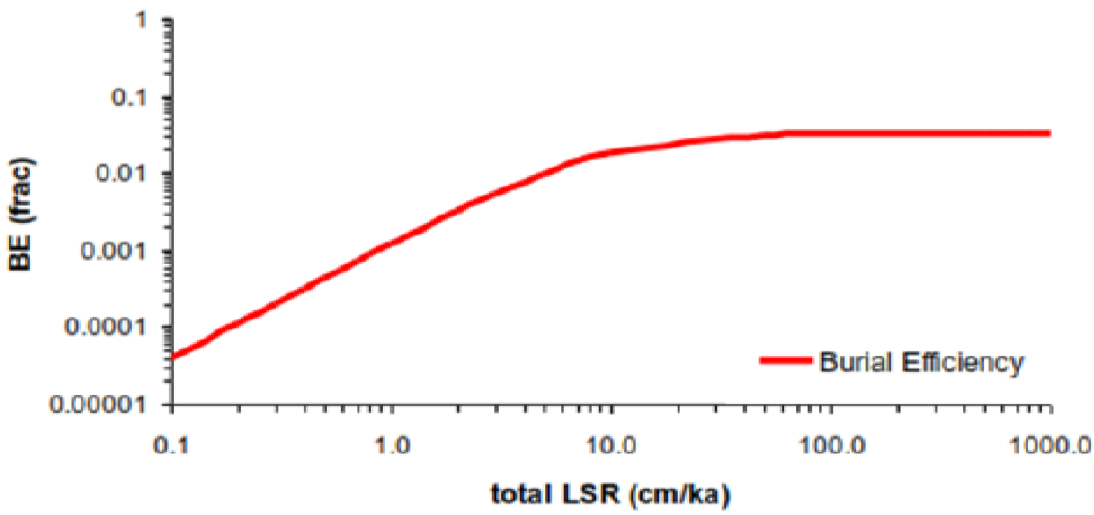


Figure 6 Burial efficiency against sedimentation rates (Betts and Holland, 1991).

### 4.6 Dilution

The association of organic carbon with inorganic materials (mineral matter) triggers the effects of dilution when inorganic materials exceeds the organic carbon content (Tyson, 2001). High dilution rate results in low organic carbon concentration whereas moderate to low dilution rates result in significant organic matter enrichment (Bohacs et al., 2005). Low dilution rates are associated with distal low energy depositional settings usually dominated with fine grained sediments (Tyson, 2001). Various contradictions have been put forward by authors regarding the sedimentation rates at which dilution plays an effective role on the total organic carbon. Although earlier works of Ibach (1982) suggested dilution started with sedimentation rates as low as 1.5-4 cm/ka, later publications by Henrichs and Reeburgh (1987) suggested sedimentation rates as high as 60-100cm/ka in contrast to the former.

## 5.0 Methodology

This shows the series of steps that are taken to achieve the aims and objectives of the project. These include:

1. Measured data collection
2. Input data calculation
3. Palaeo-water depths
4. Palaeoproductivity estimations

## 5.1 Measured data collection

The measured data include total organic carbon (TOC), hydrogen index (HI), oxygen index (OI) and maturity temperature (Tmax). These data were gathered from the Norwegian Petroleum Directorate's online factpages (www.npd.no) from multiple cores drilled into the Blodøks Formation and its equivalent, the Blålange Formation. A total number of 305 wells penetrate the Blodøks Formation. Of these, 33 wells were selected for the project. The selection of wells is based on estimations of total organic carbon within the formation from the cores. At depths where multiple estimations of total organic carbon were made, an average of the total organic carbon value is used**.** Further north, the Blodøks Formation passes into the Gapeflyndre (Cenomanian), and Breiflabb (early Turonian) which are members of the Blålange Formation in the southern and northern Norwegian Sea respectively. Three wells penetrating the Blålange Formation in the Norwegian Sea and one well each for the overlying Knitvos Formation and the underlying Langebarn Formation were also included. Figure 7 shows the wells penetrating the Blodøks, Blålange, Langebarn and Knitvos Formations.

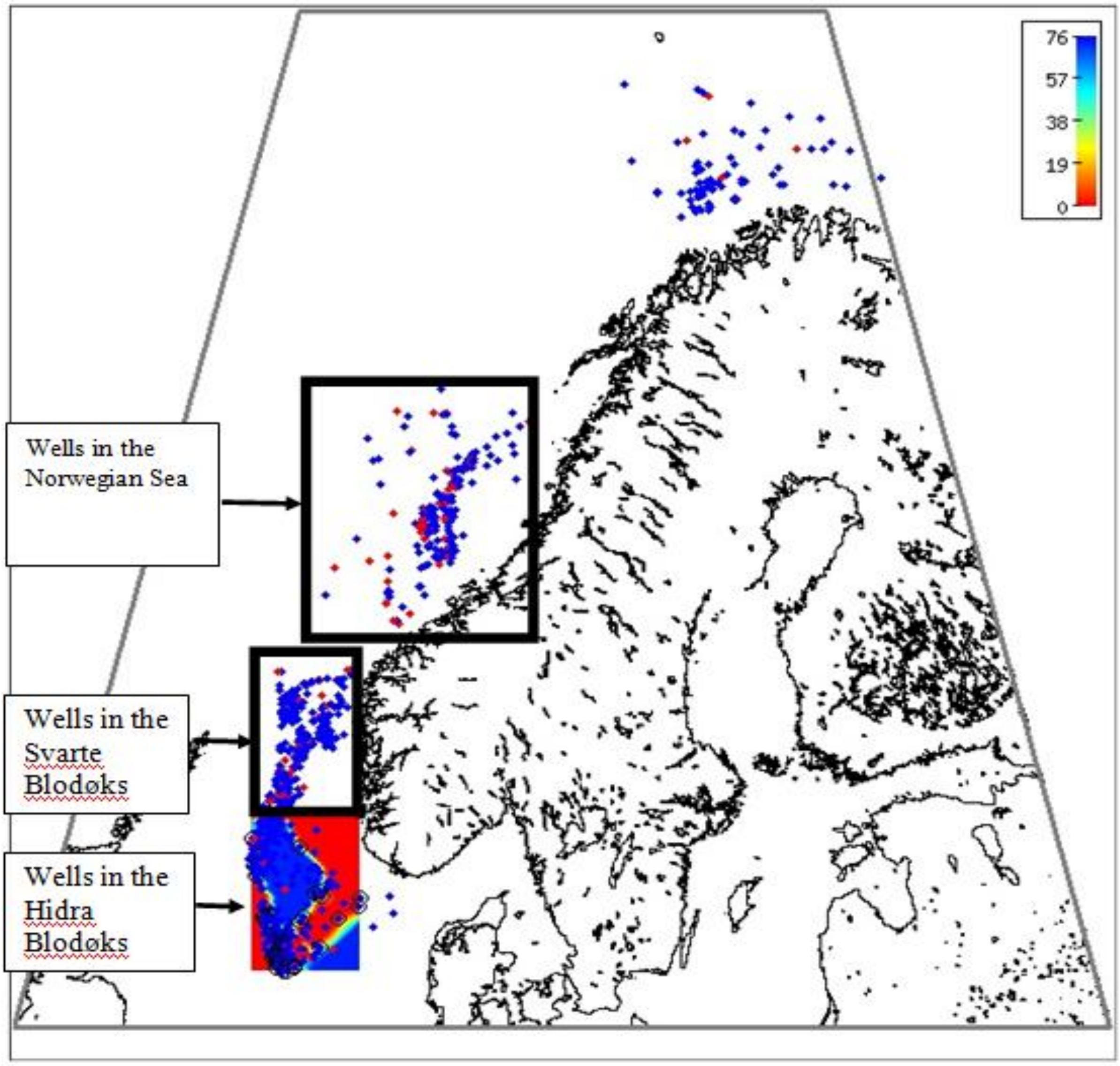


Figure 7 Map showing wells within the Hidra and Svarte Blodøks and in the Norwegian Sea (www.nhm2.uio.no/norlex).

Based on the classification of organic facies adopted by Jones (1987) as shown in Table 2, the measured organic carbon within Blodøks Formation is derived from both marine and terrestrial sources, mainly reworked organic carbon**.** The terrestrial organic carbon supplies were derived from the reduced influx of terrestrial sediments. The sources of marine organic carbon could be derived internally from the production of marine plankton in the photic zone. The dominance of reworked organic carbon suggests distant sources of organic carbon which exposed them to some level of degradation/oxidation prior to its burial at the depositional sites. From the organic carbon content (0.1-2.93 wt %), the viability of the Blodøks Formation as a potential source rock can be described as fairly good. The residual organic carbons are considered dead and incapable of producing hydrocarbons. From the maturity temperatures available, most of the organic carbon had temperatures less than 435$^0$C which is indicative of immaturity of the source rock, and a few mature within the range of 435-455$^0$C suggesting oil prone. The Blålange Formation also consisted of both highly matured and immature organic carbon.

### 5.1.1 Total organic carbon

The total organic carbon within the Blodøks Formation ranged from 0.1 to 2.93 (wt %) as shown in Figure 8 with high organic content within specific locations/areas. The measured total organic carbon from cores within the northern and southern Viking Graben (Svarte Blodøks) ranged from 0.1-2.93 wt % while cores from the Central Graben and Norwegian Danish Basin (Hidra Blodøks) ranged from 0.1-2.77 wt %.

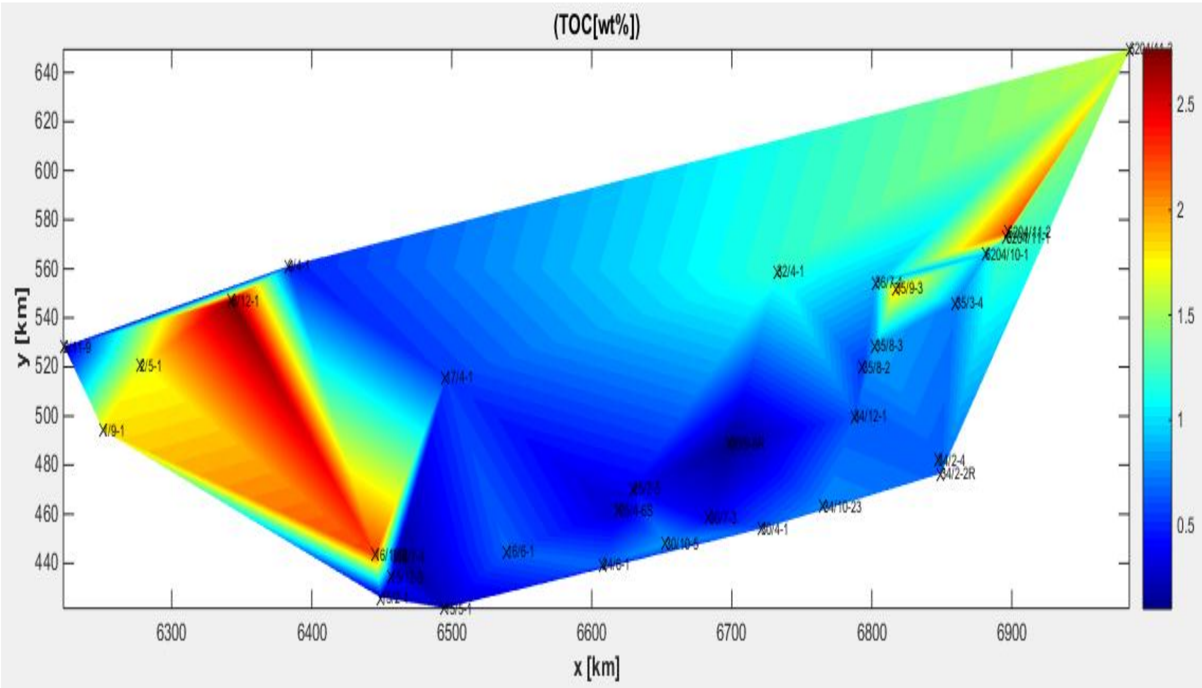


Figure 8 Spatial distribution of total organic carbon (TOC).

### 5.1.2 Hydrogen index

The averaged hydrogen indices of the entire Blodøks Formation in each core ranged from 6 to 294 (mgHC/gC) as shown in Figure 9.

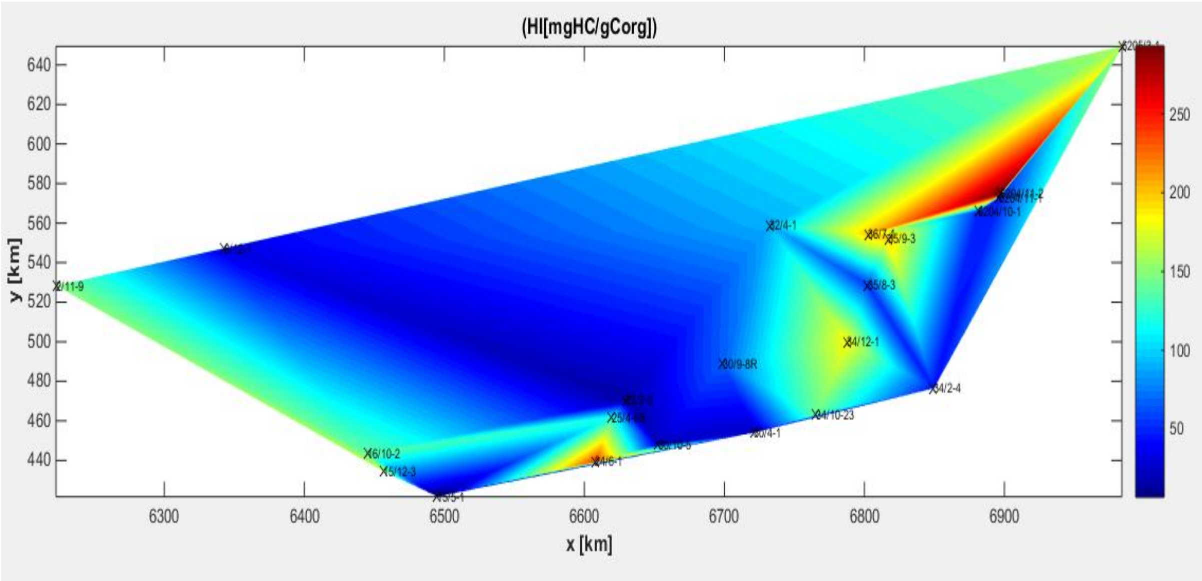


Figure 9 Spatial distribution of hydrogen index.

## 5.2 Input data calculation

The calculated input data include compacted thicknesses, compacted porosities, decompacted thicknesses, dry bulk density and sedimentation rates. The equations used for calculations are discussed below.

*Compacted thickness (m) = Bottom depth (m) – top depth (m)* ............................................*(3)*

The porosity is calculated with $\phi = \phi_0 e^{-cd}$ .........................................................*(4)*

where $\phi$ = compacted porosity (%), $\phi_0$ = initial porosity (%), $c$ = empirical compaction coefficient ($m^{-1}$), $d$ = depth (m) (Helland-Hansen et al., 1988).

This is based on shaly lithology with the assumptions that shale porosity varies as an exponential function of depth with an initial porosity of 75%, compaction coefficient of $4.4*10^{-4}m^{-1}$ and a matrix density of $2.70 g/cm^3$ (Helland-Hansen et al., 1988).

Decompacted thickness is given by $d_2 = \frac{d_1(1-\phi_1)}{(1-\phi_2)}$ ...............................................*(5)*

where $d_2$ = decompacted thickness (m), $d_1$ = compacted thickness (m), $\phi_1$ = compacted porosity (%) and $\phi_2$ = initial porosity (%) (Helland-Hansen et al., 1988).
Equation (5) is used to calculate the decompacted thickness for each core using an average of the compacted porosities calculated from equation (4) and the assumptions above.

Dry bulk density is determined as $D = \rho * (1 - \phi)$ ............................................................*(6)*

$D$ = dry bulk density ($g/cm^3$), $\rho$ = sediment density ($g/cm^3$), $\phi$ = initial porosity (%) (Dadey et al., 1992).
The dry bulk density is estimated as $0.675 g/cm^3$ using the assumptions mentioned above.

Sedimentation rate is calculated from thickness and age, $S.R = \frac{d_2}{A}$ ...............................*(7)*

$S.R$ = sedimentation rate (cm/1000yr), $d_2$ = decompacted thicknesses (cm), $A$ = age interval (Ma).
The age (time) intervals used in the calculation of the sedimentation rates of the respective formations were based on Stratigraphic Time scale by Cohen et al. (2013).
The Cenomanian to Turonian period occurred within the time interval of 100.5-89.8 (± 0.3) Ma. Since there is no exact age interval for the Blodøks Formation (Late Cenomanian to early Turonian), an age interval ranging from 96-92Ma is used to represent the Late Cenomanian and early Turonian respectively, and its equivalent in the Norwegian Sea. An average age of the interval of 4Ma is used in calculating the sedimentation rates. The interval range selected did not change the sedimentation rates much, it varied by a factor of up to 2.

The Langebarn Formation belongs to the early Cretaceous, from the Aptian to Late Albian (Færseth and Lien, 2002) which occurs within the time interval of 125-100.5Ma. Therefore an age interval of 24.5Ma is used to calculate the sedimentation rates.

The Knitvos Formation belongs to the late Cretaceous, Coniacian to late Santonian (Dalland et al. 1988). This occurs within the time interval of 89.8(±0.3) - 83.6(±0.2) Ma. An average age interval of 6.2Ma is used in calculations of the sedimentation rate.

## 5.3 Palaeo-water depth

A palaeo-water depth in the range of 400m to 500m is used for the Blodøks Formation (late Cenomanian to early Turonian). This depth interval is within the range of water depth (300m-500m) suggested by Sørensen et al. (1986) for carbonate depositions in the southern province in the North Sea during the late Cretaceous. This range interval selected is based on the fact that the Blodøks Formation is intercalated within carbonate depositions, and with the assumption that the late Cretaceous development of the North Sea is characterised by a quiescent tectonic period and so the basin configuration did not change much except for a rise in sea level (transgression)**.**

An average palaeo-water depth of 300m is used for the Langebarn Formation. This depth is within the range of the inferred water depth (100-500m) of the early Cretaceous based on micropalaeontologic reconstruction (Gillmore et al., 1999 cited in Gillmore et al., 2001). An average depth is used based on the assumption that the rise in the sea level was at its maximum in the late Cretaceous period, and therefore the water depth during the early Cretaceous is assumed to be relatively shallower than the late Cretaceous and the fact that the Cretaceous evolution in the Norwegian Sea is also a period of tectonic quiescence as suggested by Færseth and Lien (2002).

A maximum palaeo-water depth of 500m is used for the Kvitnos Formation. This water depth is the maximum limit of the inferred palaeo-water depth from the late Turonian through to the mid-Campanian ranging from 200m to 500m based on micropalaeontologic reconstruction (Gillmore et al., 1999 cited in Gillmore et al., 2001). The selected maximum depth is based on the assumption that the Kvitnos formation was deposited during the later stages of the late Cretaceous transgression where the sea level was probably at its peak.

## 5.4 Palaeoproductivity estimations

The measured data (total organic carbon), calculated data (sedimentation rate, dry bulk density) and palaeo-water depths were used as input to estimate primary productivity using the equations below.

$$PP = \frac{TOC * \rho}{0.003 * SR^{0.3}} \quad \text{.......................................................} (8)$$

$PP$ = primary productivity (gC/m$^2$/yr), $TOC$ = total organic carbon (wt %), $\rho$ = dry bulk density (g/cm$^3$), $SR$ = sedimentation rate (cm/1000yr).

Equation (8) is reordered from the Müller and Suess (1979) equation. The weakness of the Müller and Suess (1979) equation is that it does not take correction of water depth into account (Suess, 1980).

$$PP = 5.31(TOC * \rho)^{0.71} * (SR)^{0.07} * (WD)^{0.45} \quad \text{.......................................................}(9)$$

$PP$ = primary productivity (gC/m$^2$/yr), $TOC$ = total organic carbon (wt %), $\rho$ = dry bulk density (g/cm$^3$), $SR$ = sedimentation rates (cm/1000yr), $WD$ = water depth (m) (Stein, 1986)

## 6.0 Results

The measured data, calculated input data and estimated palaeoproductivity of the Blodøks, Gapeflyndre and Breiflabb (Blålange Formation), Langebarn and Knitvos Formations using the Stein (1986) equation and the Müller and Suess (1979) equation are given in Appendix 2,3,4,5 and 6 respectively.

### 6.1 Spatial distribution map of calculated input data

The spatial distribution maps of some calculated data such as compacted thicknesses, compacted porosities, sedimentation rates and primary productivity of the Blodøks Formation were generated using the Universal Transverse Mercator (UTM) coordinate system and zones of the wells gathered from the Norwegian Petroleum Directorate's online factpages (www.npd.no). The UTM coordinates expressed in kilometres were aligned within the same zone of 31 (Northern hemisphere). The input variables and their corresponding wells were interpolated onto a regular grid for plotting using Matlab codes.

#### 6.1.1 Compacted thickness

The compacted thicknesses within the Blodøks Formation ranged from 1-149m as shown in Figure 10.

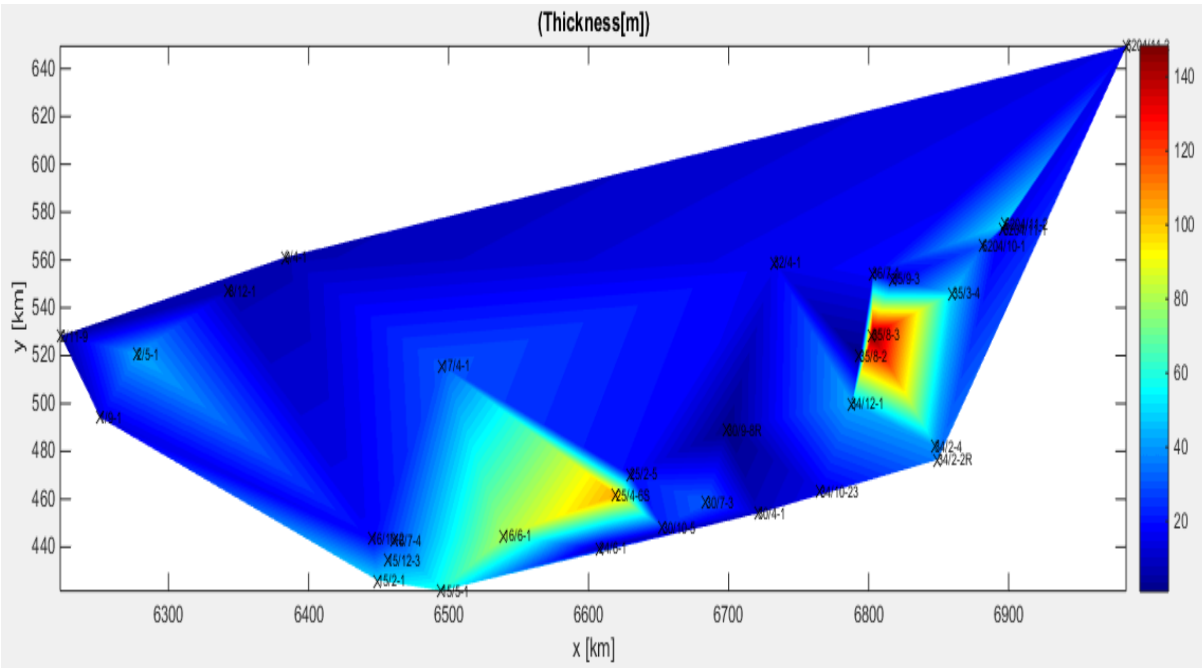


Figure 10 Spatial distribution of thickness.

### 6.1.2 Compacted porosities

The averaged compacted porosities for each Blodøks Formation core varied from 13.3% (lowest) to about 49.4% (highest). Figure 11 shows the distribution model of the compacted porosities within the Blodøks Formation. The lower porosities correlate with deeper depths at which the formation was being encountered by the wells whereas the relatively high porosities correlate with shallower depths.

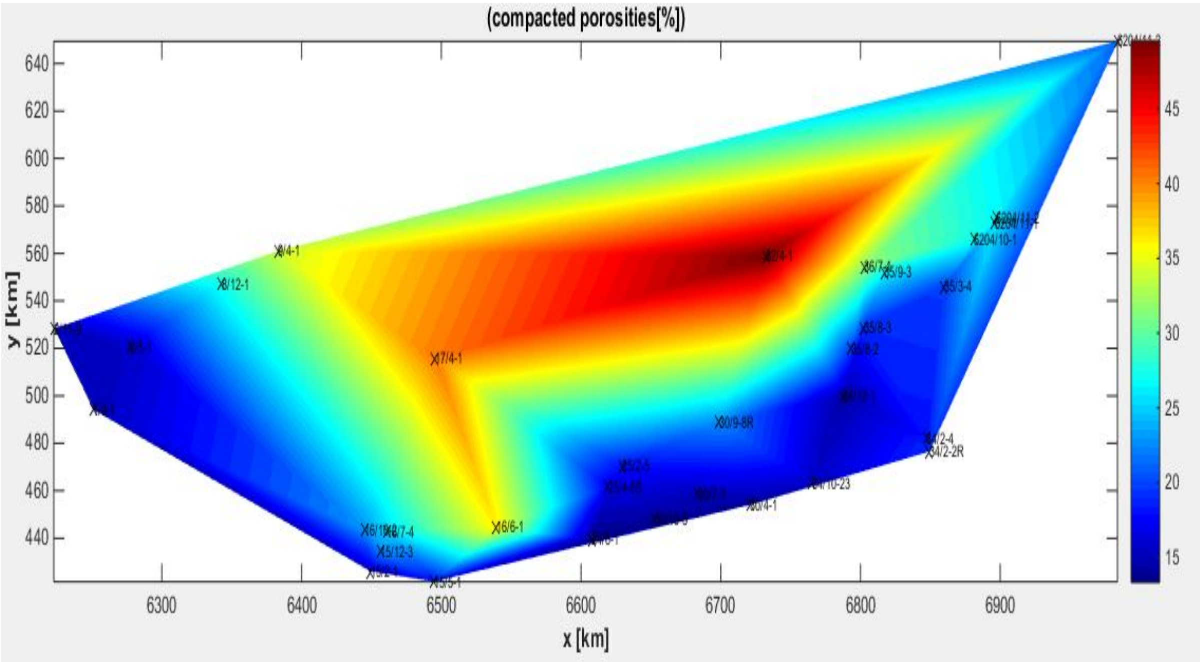


Figure 11 The distribution of compacted porosities.

### 6.1.3 Sedimentation rates

The rate at which the Blodøks Formation was being deposited can be inferred to be very low. The sedimentation rates varied from 0.08cm/1000yr (lowest) to 12.16cm/1000yr (highest) as shown in Figure 12. This is similar to Figure 10, hence the thickness of the formation increases with sedimentation rate.

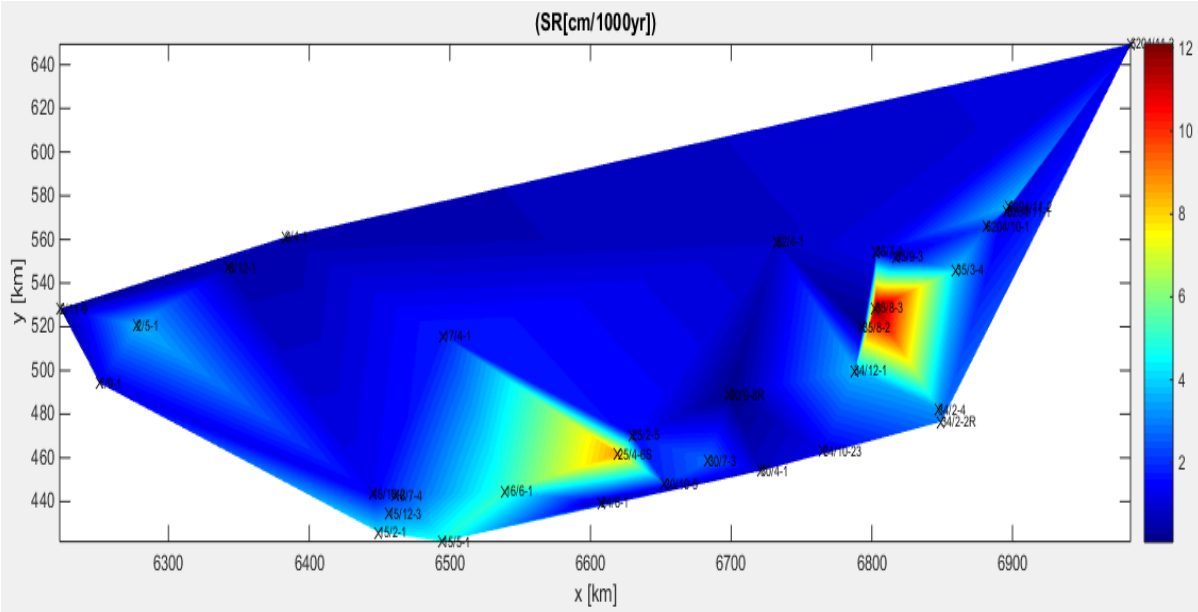


Figure 12 The distribution of sedimentation rates.

### 6.1.4 Primary productivity

With constant input variables such as sedimentation rates, dry bulk density and total organic carbon, both the Müller and Suess (1979) and Stein (1986) equations give a similar trend of increase and decrease which corresponds to the variations in the total organic carbon. Hence, at depths where the total organic carbon values were relatively high, the estimated palaeoproductivities in both cases were also high (See Appendix 2). The Müller and Suess (1979) equation results in high estimations of palaeoproductivity compared to the Stein (1986) equation, up to a factor of 2-3 with the exception of a few instances where the difference is less. The Stein (1986) equation gives an estimated range of palaeoproductivity due to inferred palaeo-water depths of 400 to 500m being used. The estimated range is very close and therefore the Stein (1986) equation result is more reliable. Also, the Stein (1986) equation considers the loss of carbon flux to degradation as a result of the water depths. Therefore the interpretation of palaeoproductivity results will be based on the Stein (1986) equation.

Figure 13 shows the distribution model of the averaged primary productivity of the Blodøks Formation for each core with relatively high primary productivity occurring at specific areas. It can be observed that the distribution of total organic carbon (Figure 8) is somewhat similar to the primary productivity map (Figure 13), hence in areas where the total organic carbon values were high, the primary productivity was also high.

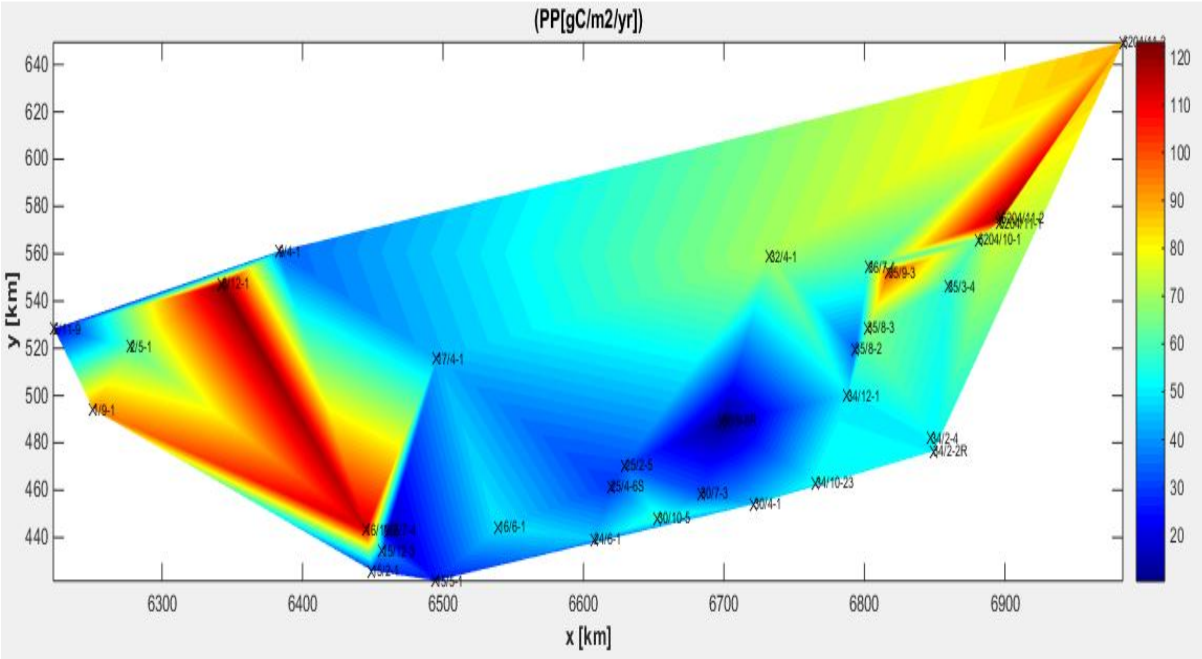


Figure 13 The distribution of primary- productivity.

### 6.2 Graphs of input variables within the Blodøks Formation

The graphs displayed in Figures 14 & 15 show the relationship between some of the input variables whereas Figures 16 & 17 show palaeoproductivity versus depth from cores. From Figure 16, it is observed that there is a slight overall decrease in productivity over time while Figure 17 shows no clear trend in productivity over time.

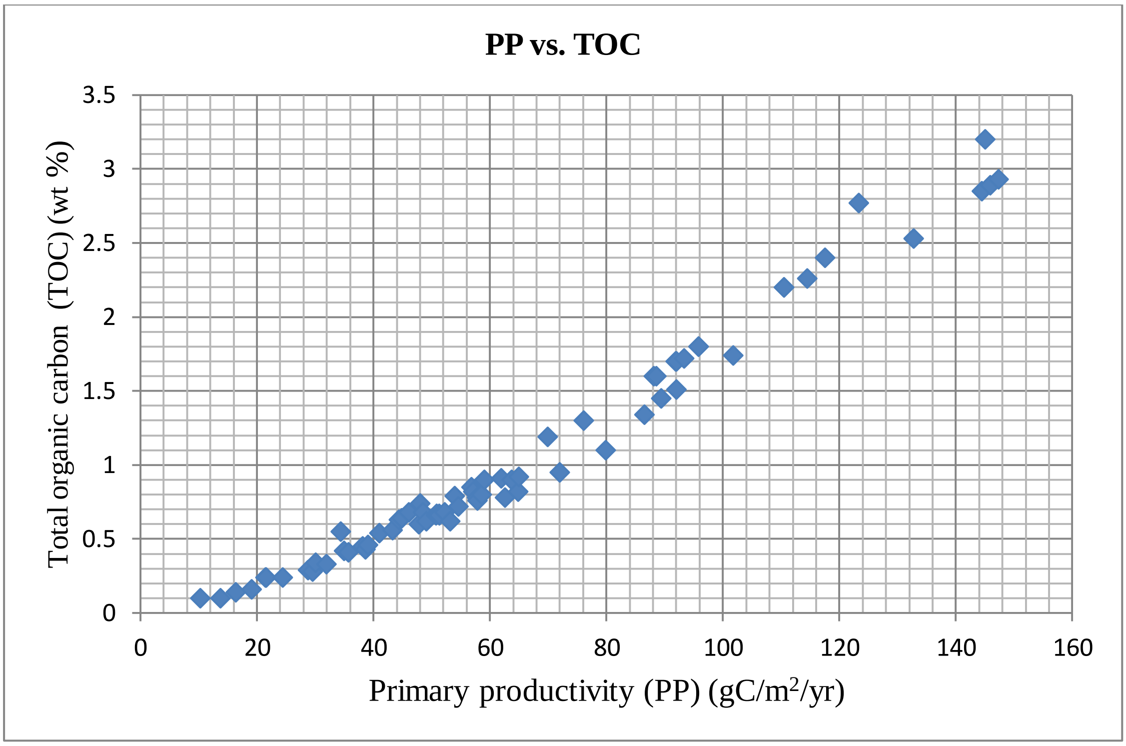


Figure 14 The relationship between total organic carbon and primary-productivity within the Blodøks Formation.

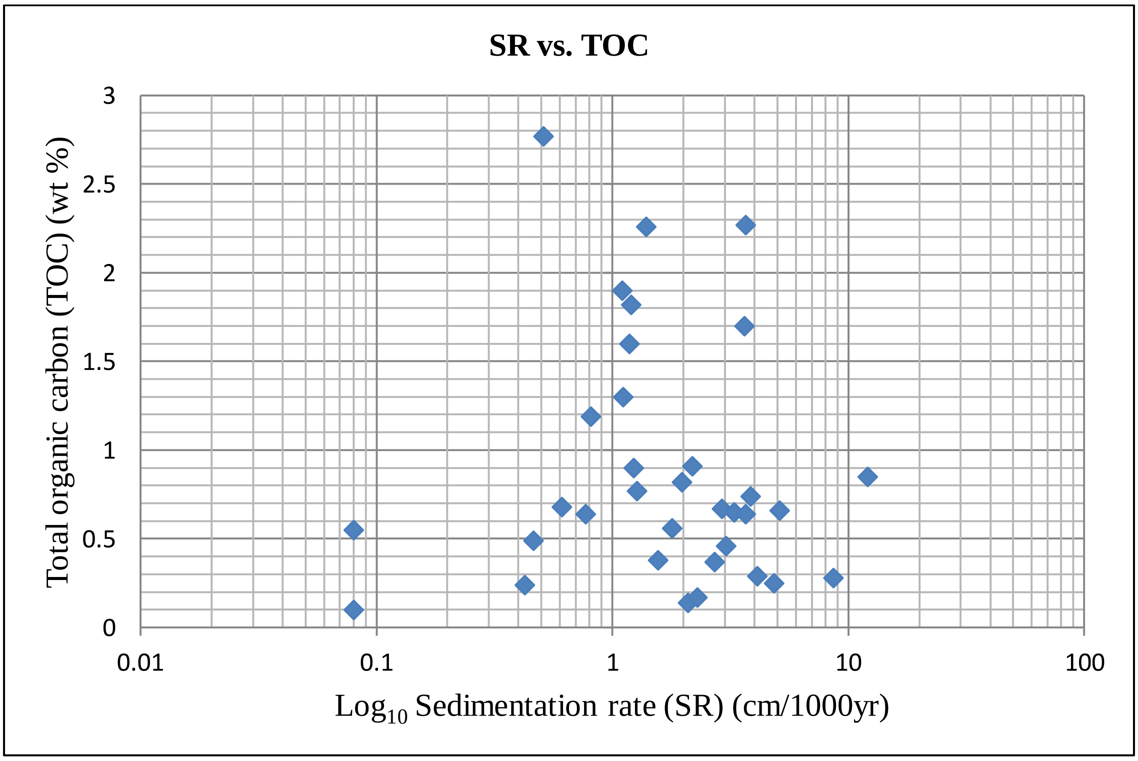


Figure 15 Sedimentation rate versus total organic carbon within the Blodøks Formation.

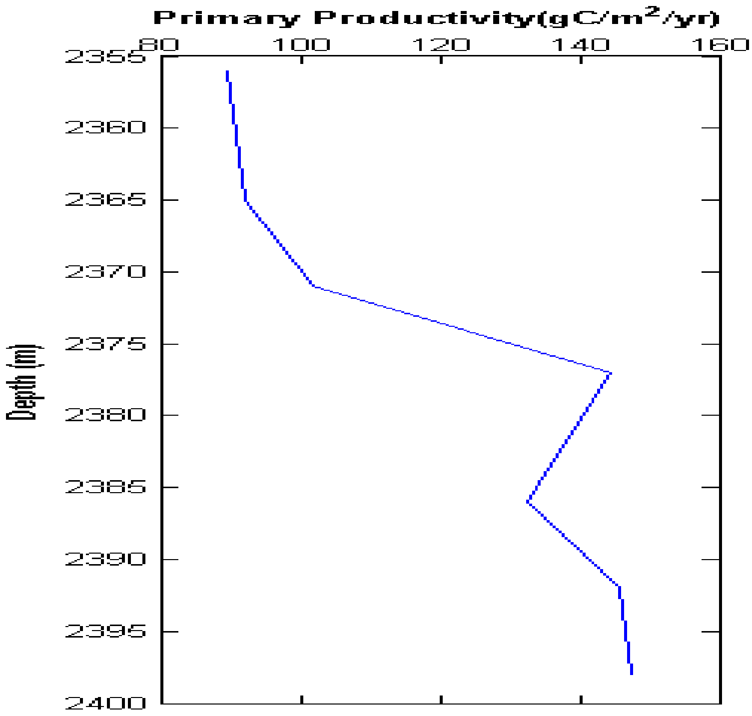


Figure 16 Primary productivity versus depth within the Blodøks Formation (core 6204/11-2).

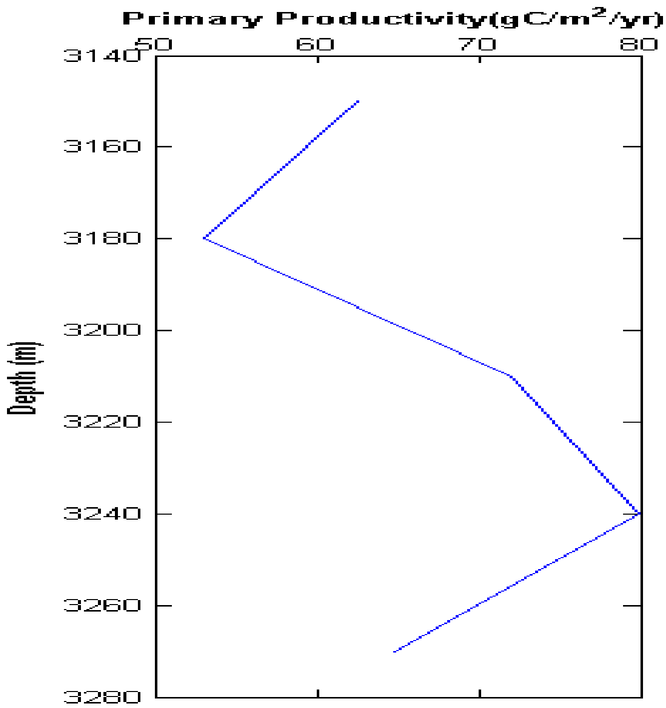


Figure 17 Primary productivity versus depth within the Blodøks Formation (core 35/8-3).

### 6.3 Graphs of input variables within the Blålange Formation

The graph displayed in Figure 18 shows the relationship between some of the input variables while Figures 19, 20 & 21 show palaeoproductivity with depth from different cores.

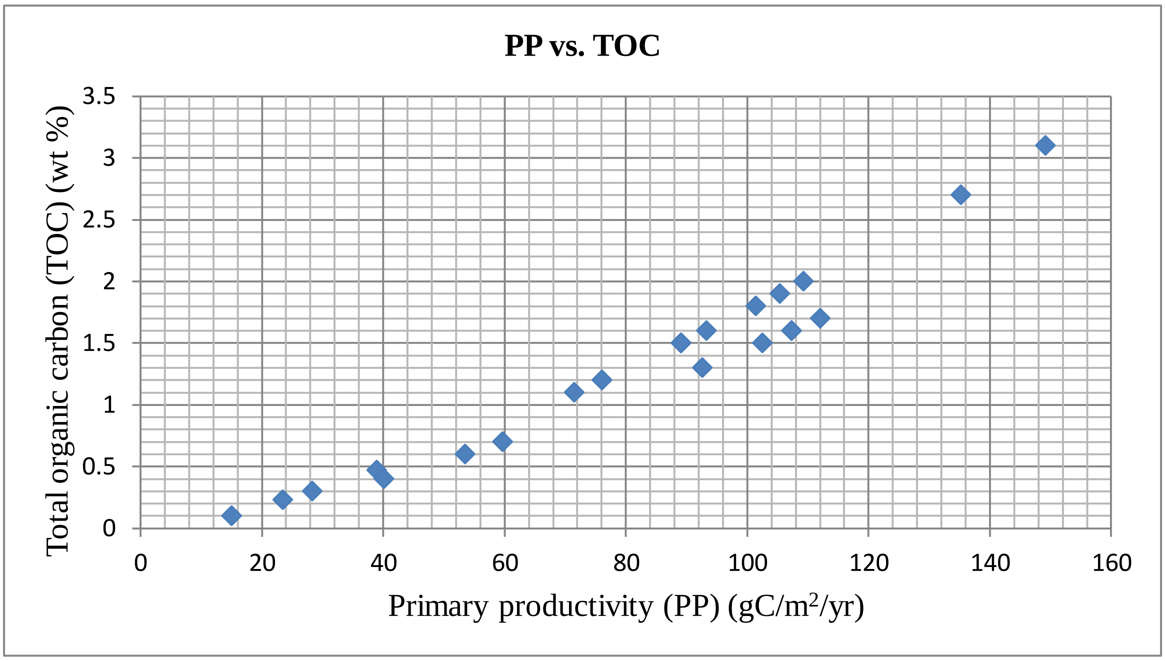


Figure 18 The relationship between primary productivity rate and total organic carbon within the Blålange Formation.

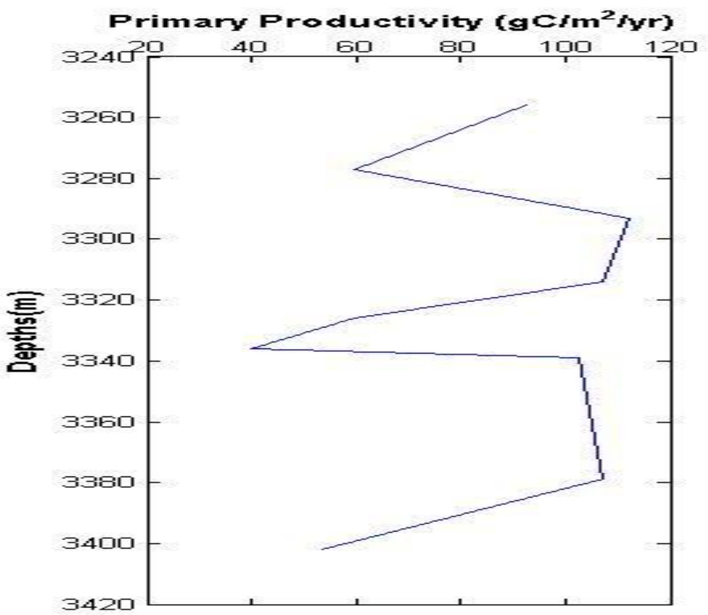


Figure 19 Primary productivity versus depth of the Gapeflyndre member (core 6305/12-1).

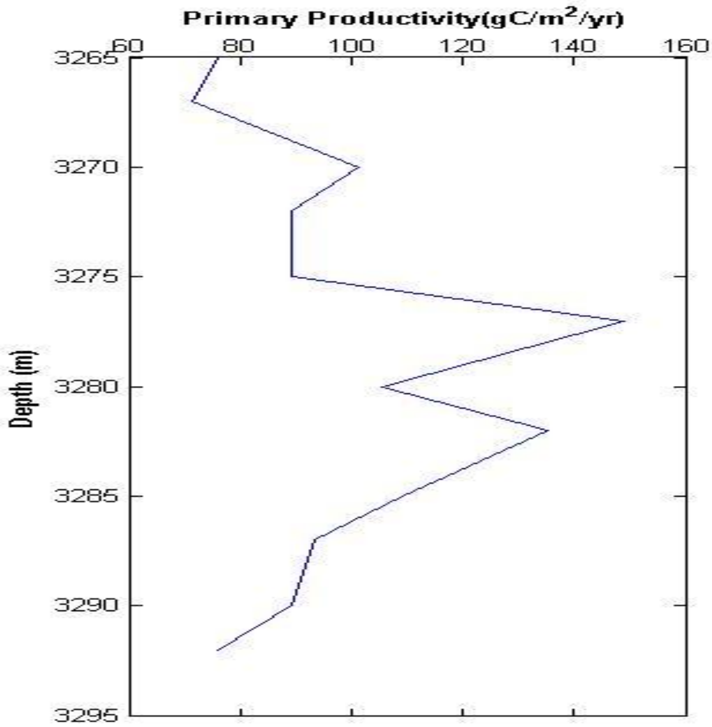


Figure 20 Primary productivity versus depth of the Breiflabb member (core 6507/2-2).

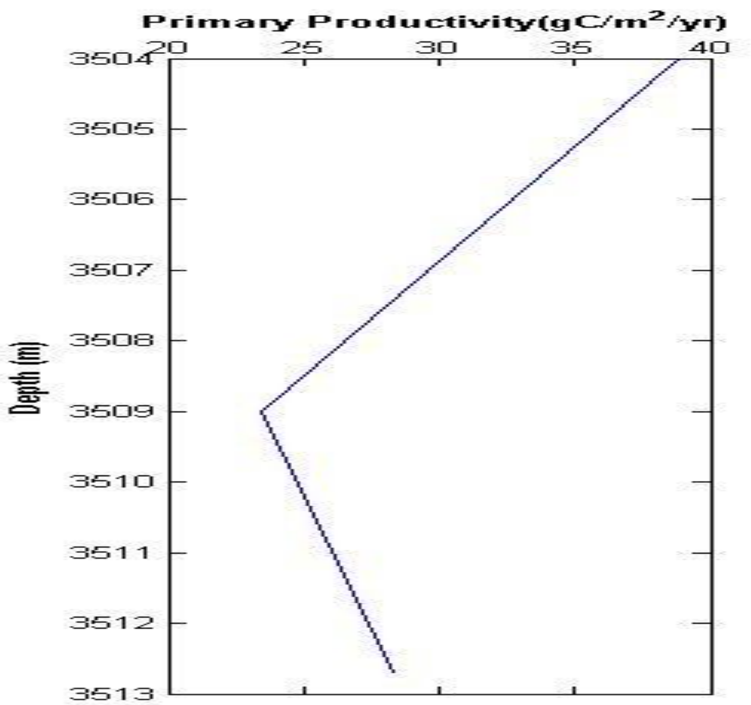


Figure 21 Primary productivity versus depth of the Breiflabb member (core 6507/7-1).

## 7.0 Discussion

The sedimentation rates within the Blodøks Formation as shown in Figure 12 are low. The low sedimentation rates give an indication of a reduced influx of terrestrial material during the time interval which is in agreement with Isaksen and Tonstad (1989). Figure 15 shows the sedimentation rates versus total organic carbon. The absence of any clear correlation indicates that the accumulation of organic carbon within the Blodøks Formation is independent of sedimentation rates. This indirectly rules out any linkage of dilution effects on the accumulated organic carbon.

The averaged primary productivity at each core depth within the Blodøks Formation ranged from 10.3-147.3 gC/$m^2$/yr (See Appendix 2). This low to moderate productivity rate gives an indication that the anoxic condition within the water column is unlikely to be controlled by primary productivity since anoxia would require much higher primary productivity rates such as in upwelling zones as suggested by Demaison and Moore (1980). The possible cause of the level of productivity may be attributed to poor circulation of water masses coupled with limited nutrient supply within the basins. This could have resulted from the isolation of the North Sea basins from the global oceanic circulation during the late Cretaceous as suggested by De Graciansky et al. (1986); hence the North Atlantic and South Atlantic oceans were constricted. In Figure 14, it is obvious that a positive correlation (linear relationship) can be observed between primary productivity and total organic carbon. This observation seems plausible due to the fact that with increasing primary productivity, the flux of organic carbon reaching the sediment-water interface increases which is subsequently preserved in the anoxic water bottom. Overall, there is no clear trend in palaeoproductivity over time in the Blodøks Formation as it varies from core to core and therefore may be attributed to local variation in productivity rates within the basin (Appendix 2; Figures 16& 17).

Also, it can be inferred that the anoxic conditions during the time interval as suggested by Jenkyns (1980) also contributed to the preservation of organic carbon. This is based on the observation that although the level of primary productivity rates within the Blodøks Formation is not specifically high (low to moderate), the total organic carbon values are moderately high. This can be explained by the fact that given the anoxic conditions at the water bottom during the time interval, the effects of bacterial degradation and scavenging by fauna could have been reduced drastically, thus enhancing organic carbon accumulation.

Figures 19, 20 & 21 show the calculated primary productivity rates with depths from cores within the Blålange Formation. It is observed from Figure 19 that the primary productivity trend did not change much over time within the Gapeflyndre whereas Figures 20 & 21 show different palaeoproductivity rates over time within the Breiflabb Formation. This may be attributed to different composition of the cores within the depth interval and therefore different depositional energy. The depths of Figure 20 are composed of sandstone/siltstone whereas Figure 21 is mainly composed of sandstones.

As seen in Figure 18, the primary productivity rates within the Blålange Formation also had a positive influence on the organic carbon content**.** Although the sedimentation rate of the Gapeflyndre member is higher than the range of the Blodøks Formation, it can be inferred that it did not affect the preservation of organic carbon since the organic carbon values are within the same range as the Blodøks Formation (See Appendix 2 & 3). It can therefore be suggested that regionally palaeo-conditions from the North Sea to the Norwegian Sea during the late Cenomanian to early Turonian period did not vary much.

In comparison of the primary productivity rates based on the Stein (1986) equation, sedimentation rates and organic carbon accumulation within the formations in the Norwegian Sea, the primary productivity rate of the Langebarn Formation (Appendix 5) and Knitvos Formation (Appendix 6) were generally low though the measured organic carbon values were moderate. Although the sedimentation rate of the Knitvos Formation is higher than the sedimentation rate of the Blålange and Langebarn, it can be inferred that organic carbon accumulation might be independent on the sedimentation rates since the total organic values did not change much compared with the Blålange Formation. The maximum total organic values of the Blålange Formation varied by a factor of up to 2. Therefore anoxia may be the primary control on the accumulation of organic carbon and locally primary productivity rate within the Langebarn and Knitvos Formation.

### 7.1 Regional correlation of the Blodøks Formation

In correlation with the Black Band Formation of UK, Barrett (1998) suggested anoxia and increased primary productivity as the main factors influencing the preservation of organic carbon within the Black Band Formation. However, the estimated palaeoproductivity of the Blodøks Formation indicates low to moderate primary productivity rate. This suggests variations in the rates of primary productivity; hence palaeoproductivity in the UK sector is likely to have been higher than in Norwegian sector of the North Sea within the time interval.

### 7.2 Limitation

Summing up, there were a number of draw-backs in this project which was kept in mind when interpreting the results but on simple bases given the information that is available, an attempt is made to regionally correlate the formation. Though the Blålange and Blodøks Formations consisted of traces of sandstones and carbonates (limestones) at certain depths respectively, it is predominantly claystone/shales and therefore the given assumptions and equations based on shaly lithology are valid. The assumed palaeo-water depths during the deposition of the formations were based on inferred water depths during the time interval coupled with the tectonic history of the basins of the time interval. The total organic carbon values do not differentiate between marine and terrigenous origin so the calculated primary productivity is a maximum value.

## 8.0 Conclusion

The estimated level of palaeoproductivity within the Blodøks Formation of the North Sea ranged from low to moderate. These were modelled to determine the spatial distribution and variations. From the results, the main factors that influenced the accumulation of organic carbon within the Blodøks Formation and its equivalent formation were the primary productivity rates and the anoxic conditions within the water column.

The cause of the primary productivity rates is assumed to be associated with poor oceanic circulation of water masses coupled with limited nutrient supply within the basins due to constriction of the North Atlantic and South Atlantic oceans during the period.

Regionally, the palaeo-depositional conditions of the Blodøks Formation (Svarte and Hidra Blodøks) of the North Sea were similar to the Blålange Formations (Gapeflyndre and Breiflabb) of the Norwegian Sea. This is supported by similar organic carbon values, sedimentation rates and primary productivity rates.

The influences on the accumulated organic carbon within the Langebarn Formation and the Knitvos Formation in the Norwegian Sea during the Cretaceous period are inferred to be controlled mainly by anoxia and locally primary productivity.

## References

Allen, P. A., & Allen, J. R. (2013). Basin analysis: Principles and application to petroleum play assessment. John Wiley & Sons.

Barrett P. (1998). A comparative organic geochemical and stable isotope study of the Cenomanian-Turonian organic-rich sediments from Tunisia, Germany and UK. Unpublished Doctoral thesis. University of New Castle upon Tyne (pp. 23-44).

Berger, WH. and Herguera, J. C. (1992). Reading the sedimentary record of the ocean's productivity. In Primary productivity and Biogeochemical cycles in the sea (pp. 455-486). Springer US.

Berger, W.H., Fischer, K., Lai, C. & Wu, G. (1987). Ocean Productivity and Organic Carbon Flux. I. Overview and Maps of Primary Production and Export Production. San Diego, Univ. California: SIO Reference, 87-30.

Berger, W. H. (1989). Productivity of the ocean: present and past. In Dahlem Workshop Report, 44. Wiley.

Betzer, P.R., Showers, W.J., Laws, E. A., Wian, C.D., di Tullio, G.R. and Kroopnick, P.M. (1984). Primary productivity and particle fluxes on a transect to the equator at 1530 W in the Pacific Ocean. Deep-Sea Res., 31(1), 1-11.

Betts, J. N., & Holland, H. D. (1991). The oxygen content of ocean bottom waters, the burial efficiency of organic carbon, and the regulation of atmospheric oxygen. Palaeogeography, Palaeoclimatology, Palaeoecology, 97(1), 5-18.

Bohacs, K. M. (2005). Production, destruction, and dilution-the many paths two source rock development. Special Publication of SEPM (Society for Sedimentary Geology), ISBN 1-56576-110-3, 61–101.

Brekke, H., Sjulstad, H. I., Magnus, C., & Williams, R. W. (2001c). Sedimentary environments offshore Norway—an overview. Norwegian Petroleum Society Special Publications, 10, 7-37.

Canfield, D. E. (1994). Factors influencing organic carbon preservation in marine sediments. Chemical Geology, 114(3), 315-329.

Christiansson, P., Faleide, J.I. and Berge, A.M. (2000). Crustal structure in the northern North Sea – An integrated geophysical study. In: Nøttvedt, A. (ed.), Dynamics of the Norwegian Margin. Geological Society Special Publication 167.

Cohen, K.M., Finney, S.C., Gibbard, P.L. & Fan, J.X. (2013; updated). The ICS International Chronostratigraphic Chart. Episodes 36: 199-204.

Dalland, A., Worsley, D., & Ofstad, K. (Eds.). (1988). A Lithostratigraphic Scheme for the Mesozoic and Cenozoic and Succession Offshore Mid-and Northern Norway . NPD.

Dadey, K. A., Janecek, T., & Klaus, A. (1992). Dry-bulk density: its use and determination. In Proceedings of the Ocean Drilling Program, Scientific Results (Vol. 126, pp. 551-554). College Station, TX.

Deegan, C. E. and Scull, B. J. (1977). A standard lithostratigraphic nomenclature for the central and northern North Sea. Report of the Institute of Geological Sciences, No. 77/25. Norwegian Petroleum Directorate Bulletin 1.

Degens, E. T., Emeis, K. C., Mycke, B., & Wiesner, M. G. (1986). Turbidites, the principal mechanism yielding black shales in the early deep Atlantic Ocean. Geological Society, London, Special Publications, 21(1), 361-376.

De Graciansky, P. C., Deroo, G., Herbin, J. P., Jacquin, T., Magniez, F., Montadert, L., & Sigal, J. (1986). Ocean-wide stagnation episodes in the Late Cretaceous. Geologische Rundschau, 75(1), 17-41.

Demaison, G. J. and G. T. Moore (1980). Anoxic environments and oil source bed genesis. Organic Geochemistry 2(1): 9-31.

Færseth, R. B., & Lien, T. (2002). Cretaceous evolution in the Norwegian Sea—a period characterized by tectonic quiescence. Marine and Petroleum Geology, 19(8), 1005-1027.

Faleide, J. I., Bjørlykke, K. and Gabrielsen, R. H. (2010). Geology of the Norwegian continental shelf. In: Bjørlykke K. (ed.), Petroleum Geoscience: From Sedimentary Environments to rock Physics. Springer Science, 467 – 499.

Felix, M. (2014). A comparison of equations commonly used to calculate organic carbon content and marine palaeoproductivity from sediment data. Marine Geology, 347, 1-11.

Gillmore, G.K., Monteil, E., Lyck, J. and Smelror, M. (1999). Tectonic impact on sedimentary processes in the post-rift phase improved models: revised biostratigraphy and paleowater depth interpretation from micropalaeontological data of selected wells in the north Viking Graben. Final report volume 2: Data documentation. IKU Petroleum Research Report 23.2561.00, 186 pp. plus appendices.

Gillmore, G. K., Kjennerud, T., & Kyrkjebø, R. (2001). The reconstruction and analysis of palaeowater depths: a new approach and test of micropalaeontological approaches in the post-rift (Cretaceous to Quaternary) interval of the Northern North Sea. Norwegian Petroleum Society Special Publications, 10, 365-381.

Glennie, K.W. and Underhill, J.R. (1998). Origin, development and evolution of structural styles. In: Glennie, K.W. (ed.), Petroleum geology of the North Sea: Basic concepts and recent advances (4th ed.). Oxford: Blackwell Science, 42-84.

Hancock, J.M. (1990) Cretaceous, In: Glennie, K.W. (ed.), Introduction to the Petroleum Geology of the North Sea Oxford: Blackwell Science, 255-272.

Hart, M. B., & Leary, P. N. (1989). The stratigraphic and palaeogeographic setting of the late Cenomanian 'anoxic'event. Journal of the Geological Society, 146(2), 305-310.

Hedges, J. I., & Keil, R. G. (1995). Sedimentary organic matter preservation: an assessment and speculative synthesis. Marine chemistry, 49(2), 81-115.

Helland-Hansen, W., Kendall, C. G. C., Lerche, I., & Nakayama, K. (1988). A simulation of continental basin margin sedimentation in response to crustal movements, eustatic sea level change, and sediment accumulation rates. Mathematical Geology, 20(7), 777-802.

Henrichs, S. M., Reeburgh, W. S. (1987). Anaerobic mineralization of marine sediment organic matter: rates and the role of anaerobic processes in the oceanic carbon economy. Geomicrobiology 5: 191- 238.

Ibach, L. E. J. (1982). Relationship between sedimentation rate and total organic carbon content in ancient marine sediments. AAPG Bulletin, 66(2), 170-188.

Isaksen, D., & Tonstad, K. (Eds.). (1989). A revised Cretaceous and Tertiary lithostratigraphic nomenclature for the Norwegian North Sea. Norwegian Petroleum Directorate.

Jenkyns, H. C. (1980). Cretaceous anoxic events: from continents to oceans. Journal of the Geological Society, 137(2), 171-188.

Jenkyns, H. C. (1985). The Early Toarcian and Cenomanian-Turonian anoxic events in Europe: comparisons and contrasts. *Geologische Rundschau, 74*(3), 505-518.

Jones, R. W. (1987). Organic facies. In : Welte D. H. (ed.). Advances in Petroleum Geochemistry 2, 1-89.

Mann U., Zweigel. J. (2008). Modelling source-rock distribution and quality variations the organic facies modelling approach. (40): 239-274.

Müller, P. J. and E. Suess (1979). Productivity, sedimentation rate, and sedimentary organic matter in the oceans—I. Organic carbon preservation." Deep Sea Research Part A. Oceanographic Research Papers 26(12): 1347-1362.

Nienhuis, P. H. (1981). Distribution of organic matter in living marine organisms.Elsevier Oceanography Series, 31 , 31-69.

Schlanger, S.0. & Jenkyns H. C. (1976). Cretaceous oceanic anoxic events: causes and consequences. Geol. Mijnbouw. 55, 179-84.

Sarnthein, M., Winn, K., Duplessy, J. C., & Fontugne, M. R. (1988). Global variations of surface ocean productivity in low and mid latitudes: influence on CO2 reservoirs of the deep ocean and atmosphere during the last 21,000 years. Paleoceanography, 3(3), 361-399.

Schlünz, B., and Schneider, R. R. (2000). Transport of terrestrial organic carbon to the oceans by rivers: re-estimating flux-and burial rates. International Journal of Earth Sciences, 88(4), 599-606.

Schwarzkopf, T. A. (1993). Model for prediction of organic carbon content in possible source rocks. Marine and petroleum geology, 10(5), 478-492.

Sørensen, S., Jones, M., Hardman, R. F. P., Leutz, W. K., & Schwartz, P. H. (1986). Reservoir characteristics of high-and low-productivity chalks from the Central North Sea. In Habitat of hydrocarbons on the Norwegian continental shelf; proceedings of an international conference: London, Graham and Trotman (pp. 91-110).

Sørensen, S., Morizot, H., & Skottheim, S. (1992). A tectonostratigraphic analysis of the southeast Norwegian North Sea Basin. Structural and tectonic modelling and its application to petroleum geology: Norwegian Petroleum Society: London, Special Publication, 1, 19-42.

Stein, R. (1986). Surface-water-palaeo-productivity as inferred from sediments deposited in oxic and anoxic deep-water environments of the Mesozoic Atlantic Ocean, in : E.T. Degens (Ed.), Biogeochemistry of Black Shales, Mitteilungen des Geologisch-Palaontologischen Instituts der Universitat Hambourg, 60, 55-60.

Stein, R. (1991). Accumulation of organic carbon in marine sediments: results from the Deep Sea Drilling Project/Ocean Drilling Program (DSDP/ODP). Springer-Verlag.

Suess, E. (1980). Particulate organic carbon flux in the oceans—surface. Nature, 288, 261.

Surlyk, F., Dons, T., Clausen, C.K. and Higham, J. (2003). Upper Cretaceous. In: Evans, D., Graham, C., Armour, A. and Bathurst, P (eds.), The Millennium Atlas: petroleum geology of the central and northern North Sea, 213-233.

Swiecicki, T., Gibbs, PB, Farrow, GE, & Coward, MP (1998). A tectonostratigraphic framework for the Mid-Norway region. Marine and Petroleum Geology , 15 (3), 245-276.

Tyson, R. V. (1996). Sequence-stratigraphical interpretation of organic facies variations in marine siliciclastic systems: general principles and application to the onshore Kimmeridge Clay Formation, UK. Geological Society, London, Special Publications, 103(1), 75-96.

Tyson, R. V. (2001). Sedimentation rate, dilution, preservation and total organic carbon: some results of a modelling study. Organic Geochemistry 32(2): 333-339.

Van Krevelen, D. W. (1984). Organic geochemistry—old and new. Organic Geochemistry 6(0): 1-10.

Weedon, G. P., Coe, A. L., & Gallois, R. W. (2004). Cyclostratigraphy, orbital tuning and inferred productivity for the type Kimmeridge Clay (Late Jurassic), Southern England. Journal of the Geological Society, 161(4), 655-666.

Woodwell, G. M., Whitaker, R. H., Reiners, W. A., Likens, G. E., Delwich, C. C., & Botkin, D. B. (1978). Biota and the world carbon budget. Science; (United States), 199(4325).

**Other resources**

Norwegian Petroleum Online factpages (www.npd.no). (Accessed January 26, 2015)

www.nhm2.uio.no/norlex (Accessed May 2, 2015; June 10, 2015).

**Appendix**

```
% Plot the productivity rate map.
% The values need to be interpolated onto a regular grid for plotting.

clear all

% read in data filey0
% first column: x coordinates [m]
% second column: y coordinates [m]
% third column: productivity rate [gC/m2/yr]
vals = load('PP.txt');

% get the individual columns, take productivity rate
x0=vals(:,1); y0=vals(:,2); z0=(vals(:,3));  % value = vals(:,4);
% create a linear space for interpolation
x=linspace(min(vals(:,1)),max(vals(:,1)),1000);
y=linspace(min(vals(:,2)),max(vals(:,2)),1000);

% create a regular grid for interpolating values
[Xinterp,Yinterp]=meshgrid(x,y);

% interpolate values between measured locations
Zinterp=griddata(x0,y0,z0,Xinterp,Yinterp);

% plot results
% contourf(Xinterp/1000,Yinterp/1000,Zinterp), axis equal, axis tight
pcolor(Xinterp/1000,Yinterp/1000,Zinterp), axis equal, axis tight
shading('flat')
colormap(jet)
colorbar
% plot well locations
hold on, plot(x0/1000,y0/1000,'xk'), hold off
% annotate plot
xlabel('x [km]','FontWeight','bold'), ylabel('y [km]','FontWeight','bold')
title('(PP[gC/m2/yr])')

% add text labels for the well positions
```

Appendix 1 Matlab code for primary productivity.

| Wells | Depth (m) | Compacted Thickness (m) | Compacted Porosity (%) | DBD g/cm$^3$ | D. thickness (m) | S.R (cm/ 1000yr) | PP (Stein equation) (gC/m$^2$/yr) | PP (Müller & Suess equation) (gC/m$^2$/yr) | Lithology Descriptions | TOC (wt %) | HI mgHC /gC | OI mgC $O_2$/g | Tmax $^0$C |
|---|---|---|---|---|---|---|---|---|---|---|---|---|---|
| 1/9-1 | 3648 - 3662 | 14 | 15.1 - 14.9 | 0.675 | 48 | 1.2 | | | | | | | |
| | 3660 A | | | | | | 137.73 - 152.27 | 681.67 | Shale-grey-black | 3.2 | | | |
| | 3660 B | | | | | | 38.93 - 43.05 | 146.17 | Shale-grey, greenish | 0.54 | | | |
| | 3660 | | | | | | 88.63 - 97.99 | 366.4 | Shale, grey-black and minor, grey-green, chalk+ shale calcareous | 1.72 | | | |
| 2/5-1 | 3551 - 3594 | 43 | 15.7 – 15.43 | 0.675 | 145 | 3.625 | | | | | | | |
| | 3554 - 3572 | | | | | | 60.46 - 66.85 | 137.6 | Pink grey chalk (oil stain) + 20% pale brown marl | 0.9 | | | |
| | 3575 - 3594 | | | | | | 55.61 - 61.49 | 122.32 | Pink grey chalk (oil stain) + 20% pale brown marl | 0.8 | | | |
| 2/11-9 | 3656 - 3661 | 5 | 15 - 14.9 | 0.675 | 17 | 0.425 | | | | | | | |
| | 3660 | | | | | | 20.34 - 22.51 | 69.8 | 100% Carbonate : white, light grey white, pink red, stained, hard<br>Trace, Shale/Claystone: dark grey | 0.24 | 150 | 433 | 391 |
| 8/12-1 | 2293 - 2300 | 7 | 27.3 – 27.26 | 0.675 | 20.4 | 0.51 | | | | | | | |
| | 2298 | | | | | | 117.09 - 129.46 | 762.76 | Medium-dark grey mudstone/shale | 2.77 | 33 | 70 | |
| 9/4-1 | 1804 - 1811 | 7 | 33.9 – 33.80 | 0.675 | 18.5 | 0.4625 | | | | | | | |
| | 1804 | | | | | | 20.48 - 22.64 | 68.05 | White/yellowish-brown chalk | 0.24 | | | |
| | 1808 | | | | | | 45.55 - 50.36 | 182.24 | White/yellowish-brown chalk + minor medium grey marl | 0.74 | | | |

| Wells | Depth (m) | Compacted Thickness (m) | Compacted Porosity (%) | DBD g/cm$^3$ | D. thickness (m) | S.R (cm/ 1000yr) | PP (Stein equation) (gC/m$^2$/yr) | PP (Müller & Suess equation) (gC/m$^2$/yr) | Lithology Descriptions | TOC (wt %) | HI mgHC /gC | OI mgC $O_2$/g | Tmax $^0$C |
|---|---|---|---|---|---|---|---|---|---|---|---|---|---|
| 15/2-1 | 3502 - 3551 | 49 | 16.1 – 15.7 | 0.675 | 164.8 | 4.12 | | | | | | | |
| | 3530 | | | | | | 27.30 - 30.18 | 42.67 | Mudstone, 20% Shale | 0.29 | | | |
| 15/5-1 | 3240 - 3299 | 59 | 18 – 17.57 | 0.675 | 194 | 4.85 | | | | | | | |
| | 3275 | | | | | | 18.10 - 20.02 | 22.42 | 65% Sandstone; white to light or, calcareous, glauconite | 0.16 | 6 | 94 | 392 |
| | | | | | | | | | 30% Marl ; light grey to medium grey, grey red, stained | | | | |
| | | | | | | | | | 5% Carbonate; light or, chalk | | | | |
| | | | | | | | | | Trace contamination; coal | | | | |
| | 3250 | | | | | | 30.26 - 33.45 | 46.26 | Light grey chalk+ 20% medium grey-red calcareous shale | 0.33 | | | |
| 15/12-3 | 2752 - 2791 | 39 | 22.3 - 22 | 0.675 | 121.4 | 3.04 | | | | | | | |
| | 2758 | | | | | | 37.08 - 41 | 74.14 | 100% Carbonate: white to light brown grey, chalk | 0.46 | 163 | 361 | 435 |
| | | | | | | | | | Trace, Shale/Claystone: grey red | | | | |
| | | | | | | | | | Trace, Shale/Claystone: light grey to light green grey | | | | |
| 16/6-1 | 1654 - 1734 | 80 | 36.2 – 34.9 | 0.675 | 206.2 | 5.16 | | | | | | | |
| | 1645-1665 | | | | | | 82.22 - 90.90 | 184.28 | White /light grey chalk + minor soft marl | 1.34 | | 102 | |

| Wells | Depth (m) | Compacted Thickness (m) | Compacted Porosity (%) | DBD g/cm$^3$ | D. thickness (m) | S.R (cm/ 1000yr) | PP (Stein equation) (gC/m$^2$/yr) | PP (Müller & Suess equation) (gC/m$^2$/yr) | Lithology Descriptions | TOC (wt %) | HI mgHC /gC | OI mgC $O_2$/g | Tmax $^0$C |
|---|---|---|---|---|---|---|---|---|---|---|---|---|---|
| | 1670-1690 | | | | | | 36.68 - 40.55 | 59.13 | White / light grey chalk + minor soft marl | 0.43 | | | |
| | 1695-1715 | | | | | | 54.96 - 60.77 | 104.52 | White / light grey chalk + minor soft marl | 0.76 | | 535 | |
| | 1720 - 1735 | | | | | | 13.02 - 14.40 | 13.75 | White / light grey chalk + 10% medium grey calcareous shale | 0.1 | | | |
| 16/7-4 | 2465-2493 | 28 | 25.4 – 25.04 | 0.675 | 83.8 | 2.10 | | | | | | | |
| | 2490 | | | | | | 15.53 - 17.17 | 25.21 | Shale, olive grey to light olive grey; dolomitic. | 0.14 | | | |
| 16/10-2 | 2698-2716 | 18 | 22.9 – 22.70 | 0.675 | 55.6 | 1.39 | | | | | | | |
| | 2700 | | | | | | 108.71 - 120.19 | 460.67 | 55% Shale/Claystone: dark grey | 2.26 | 138 | 22 | 437 |
| | | | | | | | | | 45% Shale/Claystone: medium, green grey | | | | |
| | | | | | | | | | Trace, carbonate; white | | | | |
| 17/4-1 | 1408 - 1438 | 30 | 40.4 – 39.84 | 0.675 | 71.9 | 1.80 | | | | | | | |
| | 1410 - 1430 | | | | | | 41.11 - 45.44 | 105.63 | Chalk+ light grey marl+ medium dark grey mudstone | 0.56 | | | |
| 24/6-1 | 3925 - 3932 | 7 | 13.3 – 13.29 | 0.675 | 24.3 | 0.61 | | | | | | | |
| | 3925.05 | | | | | | 43.74 - 48.36 | 177.46 | Shaly marl | 0.68 | 242 | | 448 |

| Wells | Depth (m) | Compacted Thickness (m) | Compacted Porosity (%) | DBD g/cm$^3$ | D. thickness (m) | S.R (cm/ 1000yr) | PP (Stein equation) (gC/m$^2$/yr) | PP (Müller & Suess equation) (gC/m$^2$/yr) | Lithology Descriptions | TOC (wt %) | HI mgHC /gC | OI mgC $O_2$/g | Tmax $^0$C |
|---|---|---|---|---|---|---|---|---|---|---|---|---|---|
| 25/2-5 | 3240 - 3259 | 19 | 18 – 17.88 | 0.675 | 62.40 | 1.56 | | | | | | | |
| | 3240 | | | | | | 28.55 - 31.57 | 66.95 | 80% Shale/Claystone: olive grey, medium light grey to medium dark grey, calcareous | 0.34 | 15 | 124 | 364 |
| | | | | | | | | | 20 % Shale/Claystone: grey red, brown grey, calcareous | | | | |
| | | | | | | | | | Trace, carbonate; yellowish grey | | | | |
| | | | | | | | | | Trace, Carbonate ; dark yellowish brown, dolomitic | | | | |
| | | | | | | | | | Trace, Contamination; Coal | | | | |
| | 3250 | | | | | | 33.18 - 36.68 | 82.7 | 85% Shale/Claystone: olive grey, medium light grey to medium dark grey, calcareous | 0.42 | 17 | 86 | 427 |
| | | | | | | | | | 15% Shale/Claystone; grey red, brown grey, calcareous | | | | |
| | | | | | | | | | Traces of Carbonate; yellowish grey | | | | |
| | | | | | | | | | Traces of carbonate; dark yellowish brown, dolomitic | | | | |
| | | | | | | | | | Trace, Siltstone; medium grey, calcareous | | | | |
| 25/4-6S | 3381- 3485 | 104 | 16.9 – 16.2 | 0.675 | 347.15 | 8.68 | | | | | | | |
| | 3395- 3405 | | | | | | 28.05 - 31.02 | 32.94 | Marl ; light grey silty | 0.28 | 121 | >170 | |
| 30/4-1 | 3761- 3770 | 9 | 14.3 – 14.27 | 0.675 | 30.9 | 0.77 | | | | | | | |
| | 3770 | | | | | | 42.58 - 47.08 | 155.75 | 60% Claystone, | 0.64 | 39 | 0 | 429 |

| Wells | Depth (m) | Compacted Thickness (m) | Compacted Porosity (%) | DBD g/cm$^3$ | D. thickness (m) | S.R (cm/ 1000yr) | PP (Stein equation) (gC/m$^2$/yr) | PP (Müller & Suess equation) (gC/m$^2$/yr) | Lithology Descriptions | TOC (wt %) | HI mgHC /gC | OI mgC $O_2$/g | Tmax $^0$C |
|---|---|---|---|---|---|---|---|---|---|---|---|---|---|
| | | | | | | | 42.11 - 46.56 | 153.32 | 40% Claystone, grey to dark grey, green, red brown | 0.63 | 10 | 8 | 257 |
| | | | | | | | | | Some amount of siderite and limestone; black claystone | | | | |
| 30/7-3 | 3633-3665 | 32 | 15.2 – 15.0 | 0.675 | 108.7 | 2.72 | | | | | | | |
| | 3650 | | | | | | 33.91 - 37.49 | 68.33 | 80% Shale | 0.41 | | | |
| | | | | | | | 36.23 - 40.05 | 75.00 | 10% Shale, fissile, non-calcareous, medium bluish grey | 0.45 | | | |
| | | | | | | | 23.18 - 25.63 | 40.00 | 10% Shale, fissile, non-calcareous, greyish brown. Minor limestone | 0.24 | | | |
| 30/9-8R | 2722-2723 | 1 | 22.6 – 22.63 | 0.675 | 3.1 | 0.08 | | | | | | | |
| | 2722 | | | | | | 9.73 - 10.76 | 48 | | 0.1 | 67 | 967 | 419 |
| 30/10-5 | 3782-3805 | 23 | 14.2 – 14.1 | 0.675 | 79.0 | 1.98 | | | | | | | |
| | 3790 | | | | | | 54.25 - 59.98 | 150.31 | 100% Claystone Some amount of coal additive and limestone. | 0.82 | 24 | 99 | 386 |
| 32/4-1 | 940-956 | 16 | 49.6 – 49.24 | 0.675 | 32.4 | 0.81 | | | | | | | |
| | 940 | | | | | | 66.38 - 73.40 | 285.22 | 100% Shale/Claystone: medium grey, calcareous | 1.19 | 90 | 121 | 353 |
| | | | | | | | | | Trace, carbonate : white, chalk | | | | |

| Wells | Depth (m) | Compacted Thickness (m) | Compacted Porosity (%) | DBD g/cm$^3$ | D. thickness (m) | S.R (cm/ 1000yr) | PP (Stein equation) (gC/m$^2$/yr) | PP (Müller & Suess equation) (gC/m$^2$/yr) | Lithology Descriptions | TOC (wt %) | HI mgHC /gC | OI mgC $O_2$/g | Tmax $^0$C |
|---|---|---|---|---|---|---|---|---|---|---|---|---|---|
| 34/2-2R | 3111-3147 | 36 | 19.1 – 18.8 | 0.675 | 116.7 | 2.92 | | | | | | | |
| | 3140 | | | | | | 48.29 - 53.39 | 109.3 | 95% Claystone, grey, some grading to light, dark and brownish, slightly calcareous to calcareous | 0.67 | | | |
| | | | | | | | | | 5% Limestone, white | | | | |
| 34/2-4 | 3247-3287 | 40 | 18 – 17.7 | 0.675 | 131.4 | 3.29 | | | | | | | |
| | 3250 | | | | | | 48.70-53.84 | 105.50 | 70% Shale/Claystone : medium to dark grey | 0.67 | 62 | 64 | 424 |
| | 3270 | | | | | | 48.18 - 53.27 | 103.90 | 50% Shale/Claystone : medium to dark grey | 0.66 | 30 | 60 | 425 |
| 34/10-23 | 3550-3565 | 15 | 15.7 – 15.6 | 0.675 | 50.6 | 1.27 | | | | | | | |
| | 3550 | | | | | | 53.95 - 59.65 | 178.02 | 65% Claystone, | 0.85 | 140 | | 416 |
| | | | | | | | 46.04 - 50.91 | 142.41 | 15% Shale | 0.68 | | | |
| | | | | | | | 51.22 - 56.63 | 165.45 | 10% Limestone, blocky, soft to moderate. hard, creamy fine, milky cut, pinkish grey | 0.79 | | | |
| | | | | | | | | | 10% Limestone - lignite | | | | |
| 34/12-1 | 3705-3748 | 43 | 14.7 – 14.4 | 0.675 | 146.97 | 3.67 | | | | | | | |
| | 3720 | | | | | | 49.59 - 54.83 | 103.58 | | 0.68 | | | |
| | 3740 | | | | | | 45.37 - 50.17 | 91.4 | | 0.6 | 183 | | 430 |

| Wells | Depth (m) | Compacted Thickness (m) | Compacted Porosity (%) | DBD g/cm$^3$ | D. thickness (m) | S.R (cm/ 1000yr) | PP (Stein equation) (gC/m$^2$/yr) | PP (Müller & Suess equation) (gC/m$^2$/yr) | Lithology Descriptions | TOC (wt %) | HI mgHC /gC | OI mgC $O_2$/g | Tmax $^0$C |
|---|---|---|---|---|---|---|---|---|---|---|---|---|---|
| 35/3-4 | 3040-3088 | 48 | 19.7 – 19.27 | 0.675 | 154.59 | 3.86 | | | | | | | |
| | 3040-3050 | | | | | | 54.86 - 60.66 | 117.03 | 98% Shale<br>Minor limestone and mudstone | 0.78 | | | |
| | 3050-3060 | | | | | | 51.83 - 57.31 | 108.02 | 98% Shale, minor cavings<br>Minor mudstone | 0.72 | | | |
| | 3060-3070 | | | | | | 46.61 - 51.53 | 93.02 | 98% Shale<br>Minor mudstone | 0.62 | | | |
| | 3070-3080 | | | | | | 61.68 - 68.19 | 138.03 | 98% Shale<br>Minor mudstone | 0.92 | | | |
| | 3080-3090 | | | | | | 48.73 - 53.87 | 99.03 | 98% Shale<br>Minor limestone and mudstone | 0.66 | | | |
| 35/8-2 | 3059-3060 | 1 | 19.5 – 19.51 | 0.675 | 3.22 | 0.08 | | | | | | | |
| | 3030-3060 | | | | | | 32.64 - 36.08 | 264.01 | 90% Silty claystone, grey, light grey, yery calcareous | 0.55 | | | |
| | | | | | | | | | 10% Sandy limestone, white | | | | |
| | | | | | | | | | Some amount of marl | | | | |
| 35/8-3 | 3122-3271 | 149 | 19 – 17.8 | 0.675 | 486.3 | 12.16 | | | | | | | |
| | 3150 | | | | | | 59.42 - 65.70 | 83.13 | | 0.78 | 44 | 210 | 441 |
| | 3180 | | | | | | 50.48 - 55.82 | 66.07 | | 0.62 | 39 | 450 | 446 |
| | 3210 | | | | | | 68.35 - 75.57 | 101.25 | | 0.95 | 38 | 193 | 438 |
| | 3240 | | | | | | 75.85 - 83.85 | 117.23 | | 1.1 | 82 | 188 | 437 |

| Wells | Depth (m) | Compacted Thickness (m) | Compacted Porosity (%) | DBD g/cm$^3$ | D. thickness (m) | S.R (cm/ 1000yr) | PP (Stein equation) (gC/m$^2$/yr) | PP (Müller & Suess equation) (gC/m$^2$/yr) | Lithology Descriptions | TOC (wt %) | HI mgHC /gC | OI mgC $O_2$/g | Tmax $^0$C |
|---|---|---|---|---|---|---|---|---|---|---|---|---|---|
| | 3270 | | | | | | 61.57 - 68.07 | 87.4 | | 0.82 | 74 | 393 | 426 |
| 35/9-3 | 2365-2380 | 15 | 26.5 – 26.32 | 0.675 | 44.15 | 1.10 | | | | | | | |
| | 2365 | | | | | | 87.25 - 96.46 | 371.72 | Claystone | 1.7 | 216 | | |
| | 2367 | | | | | | 83.68 - 92.53 | 349.85 | Claystone | 1.6 | 198 | | |
| | 2370 | | | | | | 87.40 - 96.60 | 371.72 | Claystone | 1.7 | 214 | | |
| | 2372 | | | | | | 90.98 - 100.59 | 393.58 | Claystone | 1.8 | 208 | | |
| | 2375 | | | | | | 104.92 - 115.99 | 481.046 | Claystone | 2.2 | 215 | | |
| | 2377 | | | | | | 111.60 - 123.40 | 415.27 | Claystone | 2.4 | 202 | | |
| | 2377.5 | | | | | | 90.98 - 100.59 | 393.58 | Claystone | 1.8 | 147 | | |
| | 2380 | | | | | | 104.92 - 115.99 | 481.05 | Claystone | 2.2 | 181 | | |
| 36/7-1 | 1958-1976 | 18 | 31.7 – 31.4 | 0.675 | 49.28 | 1.23 | | | | | | | |
| | 1975 | | | | | | 56.06 - 61.98 | 190.31 | Bulk (Siltsone + sandstone + claystone) | 0.9 | 200 | | 363 |
| 6204/10-1 | 2305-2335 | 30 | 27.2 – 26.8 | 0.675 | 87.6 | 2.19 | | | | | | | |
| | 2305 | | | | | | 58.83 - 65.04 | 161.84 | 100% Shale/Claystone: medium grey to dark grey | 0.91 | 49 | 141 | 429 |

| Wells | Depth (m) | Compacted Thickness (m) | Compacted Porosity (%) | DBD $g/cm^3$ | D. thickness (m) | S.R (cm/ 1000yr) | PP (Stein equation) $(gC/m^2/yr)$ | PP (Müller & Suess equation) $(gC/m^2/yr)$ | Lithology Descriptions | TOC (wt %) | HI mgHC /gC | OI mgC $O_2$/g | Tmax $^0C$ |
|---|---|---|---|---|---|---|---|---|---|---|---|---|---|
| 6204/11-1 | 2407-2422 | 15 | 26 – 25.8 | 0.675 | 44.5 | 1.11 | | | | | | | |
| | 2413.5 | | | | | | 72.26 - 79.90 | 283.48 | Claystone, dark green black- olive black, fissile, slightly silty, less micaceous, slightly - non calcareous, microlamination | 1.3 | 48 | | |
| 6204/11-2 | 2352-2402 | 50 | 26.6 – 26.1 | 0.675 | 147.3 | 3.68 | | | | | | | |
| | 2356 | | | | | | 84.92 – 94.00 | 220.88 | 100% Shale/Claystone: brown grey to medium dark grey | 1.45 | 294 | 101 | 356 |
| | 2365 | | | | | | 87.40 - 96.63 | 230.02 | 100% Shale/Claystone: brown black to grey black | 1.51 | 277 | 138 | 368 |
| | 2371 | | | | | | 96.66 - 106.87 | 265.05 | 100% Shale/Claystone: dark grey to grey black | 1.74 | 245 | 111 | 374 |
| | 2377 | | | | | | 137.21 - 151.70 | 434.14 | 100% Shale/Claystone: dark grey to grey black | 2.85 | 310 | 55 | 422 |
| | 2386 | | | | | | 126.08 - 139.40 | 385.4 | 100% Shale/Claystone: dark grey to grey black | 2.53 | 322 | 65 | 422 |
| | 2392 | | | | | | 138.57 - 153.21 | 440.23 | 100% Shale/Claystone: dark grey to grey black | 2.89 | 312 | 69 | 425 |
| | 2398 | | | | | | 139.93 - 154.71 | 446.32 | 90% Shale/Claystone: dark grey to grey black | 2.93 | 299 | 62 | 426 |
| | | | | | | | | | 10% Shale/Claystone: medium light grey to medium grey | | | | |

| Wells | Depth (m) | Compacted Thickness (m) | Compacted Porosity (%) | DBD $g/cm^3$ | D. thickness (m) | S.R (cm/ 1000yr) | PP (Stein equation) ($gC/m^2/yr$) | PP (Müller & Suess equation) ($gC/m^2/yr$) | Lithology Descriptions | TOC (wt %) | HI mgHC /gC | OI mgC $O_2$/g | Tmax $^0C$ |
|---|---|---|---|---|---|---|---|---|---|---|---|---|---|
| 6205/3-1 | 2876-2891 | 15 | 21.2 - 21 | 0.675 | 47.3 | 1.18 | | | | | | | |
| | 2880 | | | | | | 84.10 - 92.98 | 342.56 | Bulk (Siltstone/shale + sandstone + claystone | 1.6 | 159 | | 434 |
| | | | | | | | | | | | | | |

Appendix 2 Measured data, calculated input data and their corresponding estimated productivity of the Blodøks Formation using the Stein (1986) and Müller and Suess (1979) equations.

| Wells | Depth (m) | Compacted thickness (m) | Compacted porosity (%) | DBD ($g/cm^3$) | D. Thickness (m) | S.R (cm/1000yr) | PP. Stein equation ($gC/m^2/yr$) | PP. Muller and Suess ($gC/m^2/yr$) | TOC (wt %) | HI (mgHC/gC) | Tmax ($^0C$) | Lithology |
|---|---|---|---|---|---|---|---|---|---|---|---|---|
| 6305/12 -1 | 3230 - 3451.5 | 221.5 | 18.11 - 16.43 | 0.675 | 732.99 | 18.32 | | | | | | |
| | 3256 | | | | | | 87.93 - 97.21 | 122.25 | 1.3 | 122 | 446 | Siltstone |
| | 3277 | | | | | | 56.65 - 62.64 | 65.83 | 0.7 | 134 | | Siltstone |
| | 3293 | | | | | | 106.38 - 117.61 | 159.87 | 1.7 | 132 | 447 | Claystone |
| | 3314 | | | | | | 101.90 - 112.66 | 150.46 | 1.6 | 143 | 446 | Claystone |
| | 3326 | | | | | | 56.65 - 62.64 | 65.83 | 0.7 | 125 | 446 | Siltstone |
| | 3336 | | | | | | 38.08 - 42.10 | 37.62 | 0.4 | 133 | | Sandstone |
| | 3339 | | | | | | 97.33 - 107.61 | 141.06 | 1.5 | 84 | 445 | Claystone |
| | 3379 | | | | | | 101.90 - 112.66 | 150.46 | 1.6 | 129 | 447 | Claystone |
| | 3402 | | | | | | 50.78 - 56.15 | 56.42 | 0.6 | 98 | 447 | Claystone |
| | 3411 | | | | | | 14.23 - 15.734 | 9.4 | 0.1 | 207 | | Sandstone |
| | 3421 | | | | | | 14.23 - 15.734 | 9.4 | 0.1 | 75 | | Sandstone |

Appendix 3 Measured data, calculated input data and  estimated palaeoproductivity from of the Gapeflyndre member of the Blålange Formation using the Stein (1986) and Müller and Suess (1979) equations..

| Wells | Thickness (m) | Compacted Thickness (m) | Compacted Porosity (%) | DBD g /cm$^3$ | D. Thickness (m) | S.R (cm/1000 yr) | PP. Stein gC/m$^2$/yr | PP. Muller & Suess (gC/m$^2$/yr) | TOC (wt%) | HI (mgHC/gC) | OI (mgC0$_2$/gC) | Tmax ($^0$C) | Lithology |
|---|---|---|---|---|---|---|---|---|---|---|---|---|---|
| 6507/ 7-1 | 3495.5 - 3523 | 27.5 | 16.11 - 15.92 | 0.675 | 92.4 | 2.31 | | | | | | | |
| | 3504 | | | | | | 36.94 - 40.84 | 82.26 | 0.47 | 187 | 170 | 409 | Sandstone/siltstone Light grey to light dark brown |
| | 3509 | | | | | | 22.24 - 24.59 | 40.26 | 0.23 | 178 | 74 | 395 | Sandstone/siltstone Light grey to light dark brown |
| | 3512.7 | | | | | | 26.86 - 29.69 | 52.51 | 0.3 | 197 | 50 | 378 | Sandstone/siltstone Light grey to light dark brown |
| 6507/ 2-2 | 3263 - 3293 | 30 | 17.85 - 17.61 | 0.675 | 98.72 | 2.47 | | | | | | | |
| | 3265 | | | | | | 72.20 - 79.83 | 205.85 | 1.2 | 96 | | 441 | |
| | 3267 | | | | | | 67.87 - 75.04 | 188.7 | 1.1 | 105 | | 440 | |
| | 3270 | | | | | | 96.29 - 106.46 | 308.78 | 1.8 | 109 | | 434 | |
| | 3272 | | | | | | 84.59 - 93.53 | 257.31 | 1.5 | 106 | | 439 | |
| | 3275 | | | | | | 84.59 - 93.53 | 257.31 | 1.5 | 101 | | 442 | Sandstone |
| | 3277 | | | | | | 141.64 - 156.60 | 531.78 | 3.1 | 99 | | 441 | Sandstone |
| | 3280 | | | | | | 100.05 - 110.62 | 325.93 | 1.9 | 106 | | 440 | Sandstone |

| Wells | Thickness (m) | Compacted Thickness (m) | Compacted Porosity (%) | DBD g /cm$^3$ | D. Thickness (m) | S.R (cm/1000 yr) | PP. Stein gC/m$^2$/yr | PP. Muller & Suess (gC/m$^2$/yr) | TOC (wt%) | HI (mgHC/gC) | OI (mgC0$_2$/gC) | Tmax ($^0$C) | Lithology |
|---|---|---|---|---|---|---|---|---|---|---|---|---|---|
| | 3282 | | | | | | 128.41 - 141.97 | 463.17 | 2.7 | 96 | | 443 | Sandstone |
| | 3285 | | | | | | 103.76 - 114.72 | 343.09 | 2 | 93 | | 443 | Sandstone |
| | 3287 | | | | | | 88.56 - 97.92 | 274.47 | 1.6 | 87 | | 435 | Sandstone |
| | 3290 | | | | | | 84.59 - 93.53 | 254.31 | 1.5 | 120 | | 435 | Sandstone |
| | 3292 | | | | | | 72.20 - 79.83 | 205.85 | 1.2 | 125 | | 441 | Sandstone |

Appendix 4 Measured data, calculated input data and estimated palaeoproductivity from the cores within the Breiflabb member of the Blålange Formation using the Stein (1986) and Müller and Suess (1979) equations.

.

| Well | Depth (m) | Thickness (m) | Compacted Porosity (%) | DBD g/cm3 | D. Thickness (m) | S.R cm/1000yr | PP. Stein $gC/m^2/yr$ | PP. Muller & Suess $gC/m^2/yr$ | TOC wt % | Lithology | HI (mgHC/gC) | OI $mgCO_2/gC$ | Tmax $^0C$ |
|---|---|---|---|---|---|---|---|---|---|---|---|---|---|
| 6506/ 12-4 | 3835 - 3755.5 | 79.5 | 13.87 - 14.37 | 0.675 | 273.1 | 1.1 | | | | | | | |
| | 3760-3770 | | | | | | 49.25 | 198.97 | 0.91 | 55% Mudstone, | 31.79 | 156 | 430 |
| | | | | | | | 48.09 | 192.42 | 0.88 | 30% Shale | | | |
| | | | | | | | 48.87 | 196.79 | 0.9 | 15% Silty mudstone, blocky, moderate hard, non-calcareous, medium dark grey | | | |
| | 3770-3780 | | | | | | 50.77 | 207.72 | 0.95 | 60% Shale, platy to subfissile, moderate hard, non-calcareous, medium dark grey | 45.3 | 52.6 | 437 |
| | | | | | | | 42.52 | 161.81 | 0.74 | 40% Mudstone, blocky, soft to moderate hard, non-calcareous, medium grey. Minor sand and other mudstone | | | |
| | 3780-3790 | | | | | | 48.09 | 192.42 | 0.88 | 55% Shale, | 22.7 | 69.3 | 437 |
| | | | | | | | 44.94 | 174.93 | 0.8 | 45% Mudstone, minor sand, pyrites and other mudstone. LCM - lignite | | | |
| | 3790-3800 | | | | | | 45.34 | 177.11 | 0.81 | 50% Shale | 24.7 | 58 | 436 |
| | | | | | | | 43.74 | 168.37 | 0.77 | 40% Shaly mudstone, blocky to subfissile soft to moderate hard, non-calcareous, medium grey to medium olive grey | | | |
| | | | | | | | | | | 10% LCM - lignite | | | |

| Well | Depth (m) | Thickness (m) | Compacted Porosity (%) | DBD g/cm3 | D. Thickness (m) | S.R cm/1000yr | PP. Stein $gC/m^2/yr$ | PP. Muller & Suess $gC/m^2/yr$ | TOC wt % | Lithology | HI (mgHC/gC) | OI $mgCO_2/gC$ | Tmax $^0C$ |
|---|---|---|---|---|---|---|---|---|---|---|---|---|---|
| | 3800-3810 | | | | | | 44.94 | 174.93 | 0.8 | 65% Shale, platy to thinly fissile, hard, non-calcareous, medium dark grey | 18.7 | 75 | 436 |
| | | | | | | | 40.05 | 148.69 | 0.67 0.69 | 30% Shaly mudstone, | | | |
| | | | | | | | 17.39 | 45.92 | 0.21 | 5% Shale, platy, moderate hard, non-calcareous, greyish red Minor other mudstone. Minor lignite. | | | |
| | 3810-3820 | | | | | | 48.48 | 194.61 | 0.89 | 70% Shale, platy to thinly fissile, moderate hard, non-calcareous, medium dark grey | 30.7 | 113.6 | 434 |
| | | | | | | | 48.09 | 192.42 | 0.88 | 30% Shaly mudstone, blocky to subfissile, soft to moderate hard, non-calcareous, medium grey to medium olive grey. Minor other shale and mudstone | | | |
| | 3820-3830 | | | | | | 51.15 | 209.91 | 0.96 | 65% Shale | 29.2 | 45.8 | 439 |
| | | | | | | | 40.67 | 151.97 | 0.69 0.70 | 20% Shaly mudstone | | | |
| | | | | | | | 20.79 | 59.04 | 0.27 | 15% Shaly mudstone, subfissile, soft to moderate hard, non-calcareous, greyish red. | | | |

Appendix 5 Measured data, calculated input data and estimated productivity of the Langebarn Formation using the Stein (1986) and Müller and Suess (1979) equations.

| Well | Depth (m) | Thickness (m) | Compacted porosity (%) | DBD ($g/cm^3$) | D. Thickness (m) | S.R cm/1000 yr | PP. Stein $gC/m^2/yr$ | Muller & Suess gC/m2/yr | TOC wt % | Lithology | HI (mgHC/gC) | OI ($mgCO_2$/ gC) | Tmax ($^0C$) |
|---|---|---|---|---|---|---|---|---|---|---|---|---|---|
| 6506/12 -4 | 3132.5 -2600 | 532.5 | 18.9 - 23.89 | 0.675 | 1674.2 | 27 | | | | | | | |
| | 2630 | | | | | | 74.50 | 71.99 | 0.86 | 85% Shaly mudstone, blocky to subfissile soft to moderate hard, non-calcareous, medium grey | 53.5 | 166.3 | 428 |
| | | | | | | | 58.37 | 51.06 | 0.61 | 15% Silty mudstone | | | |
| | 2659 | | | | | | 57.69 | 50.22 | 0.6 | 65% Silty mudstone, blocky, soft, non-calcareous, medium light grey to light grey | 60 | 343.3 | 425 |
| | | | | | | | 72.64 | 69.48 | 0.82 0.84 | 35% Mudstone, blocky, soft, non-calcareous, medium grey | | | |
| | 2679.5 | | | | | | 58.37 | 51.06 | 0.61 | 98% Siltstone, blocky, soft, non-calcareous, grades to silty sandstone, light grey to light greenish grey | 55.7 | 141 | 426 |
| | 2690-2700 | | | | | | 71.39 | 67.8 | 0.81 | 50% Silty mudstone/siltstone, blocky, soft, non-calcareous, light grey | 71.6 | 166.7 | 430 |
| | | | | | | | 77.54 | 76.18 | 0.91 | 50% Shaly mudstone, subfissile to blocky, soft, silty, non-calcareous medium grey | | | |
| | | | | | | | | | | Minor limestone | | | |
| | 2710-2720 | | | | | | 81.14 | 81.2 | 0.97 | 60% Shaly mudstone, | 67 | 162.9 | 429 |
| | | | | | | | 77.85 | 76.59 | 0.91 0.92 | 40% Silty mudstone | | | |

| Well | Depth (m) | Thickness (m) | Compacted porosity (%) | DBD ($g/cm^3$) | D. Thickness (m) | S.R cm/1000 yr | PP. Stein $gC/m^2/yr$ | Muller & Suess gC/m2/yr | TOC wt % | Lithology | HI (mgHC/gC) | OI ($mgCO_2$/ gC) | Tmax ($^0C$) |
|---|---|---|---|---|---|---|---|---|---|---|---|---|---|
| | | | | | | | | | | Minor limestone | | | |
| | 2750-2760 | | | | | | 81.14 | 81.2 | 0.97 | 70% Shaly mudstone, | 67 | 170.1 | 428 |
| | | | | | | | 72.02 | 68.64 | 0.82 | 30% Silty mudstone | | | |
| | | | | | | | | | | Minor other caved mudstone | | | |
| | 2780.5 | | | | | | 55.63 | 47.71 | 0.57 | 98% Shaly mudstone, subfissile, soft to moderate hard, non-calcareous, silty, medium grey | 26.3 | 45.6 | 423 |
| | 2780-2790 | | | | | | 73.88 | 71.15 | 0.85 | 50% Silty mudstone, blocky, soft to moderate hard, non-calcareous, medium grey | 58.8 | 142.4 | 430 |
| | | | | | | | 79.35 | 78.69 | 0.93<br>0.95 | 50% Shaly mudstone, subfissile to blocky soft to moderate hard, non-calcareous, medium dark grey | | | |
| | 2800-2810 | | | | | | 70.77 | 66.97 | 0.8 | 50% Silty mudstone, | 71.1 | 154.6 | 427 |
| | | | | | | | 81.14 | 81.2 | 0.97 | 50% Shaly mudstone | | | |
| | 2840 | | | | | | 76.33 | 74.5 | 0.89 | 60% Silty mudstone, | 64 | 202.2 | 427 |
| | | | | | | | 88.15 | 91.24 | 1.09 | 40% Shaly mudstone | | | |
| | 2870-2880 | | | | | | 75.11 | 72.83 | 0.87 | 55% Silty mudstone | 69.3 | 148.5 | 426 |
| | | | | | | | 83.50 | 84.55 | 1.01 | 45% Shaly mudstone | | | |
| | 2879.5 | | | | | | 66.31 | 61.11 | 0.73 | 98% Mudstone, subfissile, soft, silty, non-calcareous, with minor siltstone laminations, medium grey | 71.2 | 174 | 428 |

| Well | Depth (m) | Thickness (m) | Compacted porosity (%) | DBD ($g/cm^3$) | D. Thickness (m) | S.R cm/1000 yr | PP. Stein $gC/m^2/yr$ | Muller & Suess gC/m2/yr | TOC wt % | Lithology | HI (mgHC/gC) | OI ($mgCO_2$/ gC) | Tmax ($^0C$) |
|---|---|---|---|---|---|---|---|---|---|---|---|---|---|
| | 2900-2910 | | | | | | 80.55 | 80.36 | 0.96 | 60% Mudstone, subfissile to blocky, soft, silty, non-calcareous, medium dark grey to medium grey | 51.2 | 164.6 | 428 |
| | | | | | | | 75.72 | 73.66 | 0.88 | 40% Mudstone, silty, blocky, soft, non-calcareous medium light grey<br>Minor sand | 60.2 | 151.1 | 429 |
| | 2934.5 | | | | | | 62.40 | 56.09 | 0.66<br>0.68 | 98% Mudstone, subfissile to blocky, soft non-calcareous, minor siltstone laminations, medium grey | 38.8 | 92.5 | 425 |
| | 2930-2940 | | | | | | 73.26 | 70.32 | 0.84 | 75% Silty mudstone, grading in part to siltstone, blocky, soft, non-calcareous, light grey | 46.4 | 128.6 | 429 |
| | | | | | | | 78.75 | 77.85 | 0.93 | 25% Shale, platy, moderate hard, non-calcareous, medium grey<br>Minor other caved mudstone | | | |
| | 2964.5 | | | | | | 66.96 | 61.94 | 0.74 | 98% Shale, subfissile, hard, non-calcareous, medium dark grey | 16.2 | 159.5 | 353 |
| | 2960-2970 | | | | | | 66.96 | 61.94 | 0.74 | 70% Silty mudstone | 55.4 | 126.1 | 430 |
| | | | | | | | 78.15 | 77.01 | 0.90<br>0.94 | 30% Shaly mudstone | | | |
| | | | | | | | | | | Minor siltstone/sandstone | | | |
| | 2990-3000 | | | | | | 81.14 | 81.2 | 0.97 | 85% Silty mudstone, blocky, soft, non-calcareous to siltstone, medium light grey | 94.8 | 104.1 | 431 |

| Well | Depth (m) | Thickness (m) | Compacted porosity (%) | DBD ($g/cm^3$) | D. Thickness (m) | S.R cm/1000 yr | PP. Stein $gC/m^2/yr$ | Muller & Suess gC/m2/yr | TOC wt % | Lithology | HI (mgHC/gC) | OI ($mgCO_2$/ gC) | Tmax ($^0C$) |
|---|---|---|---|---|---|---|---|---|---|---|---|---|---|
| | | | | | | | 79.95 | 79.52 | 0.95 | 15% Shaly mudstone, subfissile, soft to moderate hard, non-calcareous, medium grey | | | |
| | 3020-3030 | | | | | | 76.94 | 75.34 | 0.9 | 50% Shale, platy to fissile, mod. hard, non-calcareous, medium dark grey | 50 | 84.4 | 429 |
| | | | | | | | 60.40 | 53.57 | 0.64 | 50% Silty mudstone, blocky, soft, non calc., grades to siltstone, medium light grey | 25.0 | 179.7 | 424 |
| | 3050-3060 | | | | | | 82.91 | 83.71 | 1 | 70% Silty mudstone, | 74.0 | 108 | 436 |
| | | | | | | | 79.05 | 78.26 | 0.93 0.94 | 30% Shale | | | |
| | | | | | | | | | | 10% LCM - lignite Minor siltstone and other mudstone | | | |
| | 3084.5 | | | | | | 70.77 | 66.96 | 0.8 | 98% Silty mudstone, subfissile, soft ,non-calcareous, medium grey to medium olive grey | 48.7 | 118.7 | 431 |
| | 3080-3090 | | | | | | 82.91 | 83.71 | 1 | 75% Silty mudstone, blocky, soft non-calcareous, medium light grey | 74.0 | 95 | 432 |
| | | | | | | | 82.91 | 83.71 | 1 | 25% Shale | | | |
| | | | | | | | | | | Minor LCM - lignite | | | |
| | 3100-3110 | | | | | | 92.69 | 97.94 | 1.17 | 90%Shaly mudstone, subfissile, soft, non-calcareous, medium dark grey | 92.3 | 73.5 | 434 |
| | | | | | | | | | | 10% Silty mudstone | | | |

| Well | Depth (m) | Thickness (m) | Compacted porosity (%) | DBD ($g/cm^3$) | D. Thickness (m) | S.R cm/1000 yr | PP. Stein $gC/m^2/yr$ | Muller & Suess gC/m2/yr | TOC wt % | Lithology | HI (mgHC/gC) | OI ($mgCO_2$/ gC) | Tmax ($^0C$) |
|---|---|---|---|---|---|---|---|---|---|---|---|---|---|
| | 3114.5 | | | | | | 102.34 | 112.59 | 1.35 1.34 | 98% Shaly mudstone, subfissile, soft to moderate hard, non-calcareous, medium dark grey | 59.0 | 32.8 | 427 |
| | 3110-3120 | | | | | | 97.15 | 104.64 | 1.25 | 80%Shaly mudstone, blocky, soft to moderate hard, non-calcareous, medium dark grey to medium grey | 84.8 | 76.8 | 436 |
| | | | | | | | | | | 20% LCM - lignite Minor other mudstone | | | |
| | 3120-3130 | | | | | | 84.09 | 85.38 | 1.02 | 40% Shale, platy to thinly fissile, moderate hard, non-calcareous, medium grey | 62.7 | 61.8 | 435 |
| | | | | | | | 66.96 | 61.94 | 0.74 | 30% Mudstone, subfissile to blocky, soft to moderate hard, non-calcareous, light grey | | | |
| | | | | | | | | | | 20% Sand, unconsolidated, medium grained, subangular to subrounded, fairly well sorted, clear, white | | | |
| | | | | | | | | | | 10% LCM - lignite and paint | | | |
| | 3131.12 | | | | | | | | | 98% Sandstone, blocky, medium grained, subrounded to subangular, well sorted, non-calcareous matrix, glauconitic, very pale milky cut, light grey to very light grey | | | |

| Well | Depth (m) | Thickness (m) | Compacted porosity (%) | DBD (g/cm$^3$) | D. Thickness (m) | S.R cm/1000 yr | PP. Stein gC/m$^2$/yr | Muller & Suess gC/m2/yr | TOC wt % | Lithology | HI (mgHC/gC) | OI (mgCO$_2$/gC) | Tmax ($^0$C) |
|---|---|---|---|---|---|---|---|---|---|---|---|---|---|
| | 3132.65 | | | | | | 112.66 | 128.91 | 1.54 | 98%Shale, platy, mod. hard, non-calcareous, medium grey to medium dark grey | 112.3 | 14.3 | 435 |

Appendix 6 Measured data, calculated input data and estimated productivity of the Knitvos Formation using the Stein (1986) and Müller and Suess (1979) equations.